

Annual Briefing 2024

CaMa-Flood progress report

By CaMa-Flood developer/user community
(Edited by Dai Yamazaki, Xudong Zhou, Gang Zhao)

Preface

We summarize the achievements and progresses of CaMa-Flood developments + applications in the years 2022-2024 in this annual briefing report. This briefing covers:

1. Summary of the CaMa-Flood development status
2. Achievement reports
 - a. Milestone papers on CaMa-Flood before 2021
 - b. Review of CaMa-Flood development papers
 - c. Review of CaMa-Flood applications papers
 - d. Introduction of new data/tool helpful for CaMa-Flood
3. Reports on related events and info on upcoming meetings.

The primary purpose of this briefing is to highlight the research using CaMa-Flood published in 2022-2024, and to make it visible among the CaMa-Flood community and beyond. As the 2025 March event is the first annual briefing, we also highlight historical milestone achievements before 2022.

The briefing meeting is planned on 14th March 2025, online on Zoom.

The tentative schedule is 8:00-10:30 PM in Japan time.

If you want to join the online briefing, [please register from Google Form](#)

(For presenting your achievement)

- **Submission of 1-2 page summary: by 28 February**

(For those who want to present, but cannot join on 14 Mar)

- **Deadline for video recorded talk: 7 March**

Program of online briefing on 14 March

note: times are in Japanese time zone (GMT +9)

[20:00 - 20:20]

1. Status of CaMa-Flood core developments [20 min]

[G1] Major Updates of CaMa-Flood in 2022-2024

Dai Yamazaki [12min]

[G2] CaMa-Flood accuracy evaluation

Xudong Zhou [8min]

2. CaMa-Flood achievement reports

[20:20-20:50]

2A: Highlight of milestone papers [6min * 4 talks]

[A1] Global Flood Risk under Climate Change / Global exposure to flooding from the new CMIP6 climate model projections

Yukiko Hirabayashi, et al. 2013, Nature Climate Change, <https://doi.org/10.1038/nclimate1911>

Yukiko Hirabayashi, et al. 2021, Scientific Reports, <https://doi.org/10.1038/s41598-021-83279-w>

[A2] The critical role of the routing scheme in simulating peak river discharge in global hydrological models

Fang Zhao, et al. 2017, Environmental Research Letters, <https://doi.org/10.1088/1748-9326/aa7250>

[A3] Local floods induce large-scale abrupt failures of road networks

Weiping Wang et al., 2019, Nature Communications, <https://doi.org/10.1038/s41467-019-10063-w>

[A4] Role of dams in reducing global flood exposure under climate change

Julien Boulange et al., 2021, Nature Communications, <https://doi.org/10.1038/s41467-020-20704-0>

[20:50-21:25]

2B: CaMa-Flood development papers [5min *6 talks]

[B1] Assimilation of transformed water surface elevation to improve river discharge estimation in a continental-scale river

Menaka Revel, et al. 2023, Hydrology & Earth System Sciences, <https://doi.org/10.5194/hess-27-647-2023>

[B2] A globally applicable framework for compound flood hazard modeling

Dirk Eilander et al., Natural Hazard & Earth System Sciences, <https://doi.org/10.5194/nhess-23-823-2023>

[B3] Inundation prediction in tropical wetlands from JULES-CaMa-Flood global land surface simulations

Toby Marthews et al., Hydrology and Earth System Sciences, 2022, <http://doi.org/10.5194/hess-26-3151-2022>

[B4] A New Generation of Hydrological Condition Simulator Employing Physical Models and Satellite-based Meteorological Data

Wenchao Ma et al., Earth and Space Science, 2024, <https://doi.org/10.1029/2023EA003228>

[B5] Multivariable Integrated Evaluation of Hydrodynamic Modeling: A Comparison of Performance Considering Different Baseline Topography Data

Prakat Modi et al., Water Resources Research, 2022, <https://doi.org/10.1029/2021WR031819>

[B6] Correction of River Bathymetry Parameters Using the Stage–Discharge Rating Curve

Xudong Zhou et al. 2022, Water Resources Research, <https://doi.org/10.1029/2021WR031226>

[21:25-22:05]

2C: CaMa-Flood application papers [5min * 7talks]

[C1] Quantifying the relative contributions of climate change and ENSO to flood occurrence in Bangladesh

Shahab Uddin, et al. 2023, Environmental Research Letters, <https://doi.org/10.1088/1748-9326/acfa11>

[C2] Uncertainty of internal climate variability in probabilistic flood simulations using d4PDF

Yuki Kita, & Dai Yamazaki, 2023, Hydrological Research Letters, <http://doi.org/10.3178/hrl.1715>

[C3] Methodology for constructing a flood - hazard map for a future climate

Yuki Kimura, et al., Hydrology and Earth System Science, 2023. <http://doi.org/10.5194/hess-27-1627-2023>

[C4] Reconstruction of long-term hydrologic change and typhoon-induced flood events over the entire island of Taiwan

Jac Stelly, Amar Deep Tiwari et al., Journal of Hydrology: Regional Studies, 2024, <http://doi.org/10.1016/j.ejrh.2024.101806>

[C5] Climate change and urban sprawl: Unveiling the escalating flood risks in river deltas with a deep dive into the GBM river delta

Shupu Wu et al., Science of the Total Environment, 2024, <http://doi.org/10.1016/j.scitotenv.2024.174703>

[C6] Substantial increase in future fluvial flood risk projected in China's major urban agglomerations

Ruijie Jiang et al. Communications Earth & Environment , 2023, <http://doi.org/10.1038/s43247-023-01049-0>

[C7] Flood risk assessment for Indian sub-continental river basins

Urmin Vegad et al. 2024, Hydrology and Earth System Sciences, <https://doi.org/10.5194/hess-28-1107-2024>

[22:05-22:25]

2D: New data/tool for CaMa-Flood [5min * 3talks]

[D1] AllocateRiverGauge tool v1.0

Yamazaki et al. 2024, GitHub, <https://github.com/global-hydrodynamics/AllocRiverGauge/>

[D2] AltiMaP: altimetry mapping procedure for hydrography data

Menaka Revel et al. 2024, Earth System Science Data, <https://doi.org/10.5194/essd-16-75-2024>

[D3] Res-CN (Reservoir dataset in China): hydrometeorological time series and landscape attributes across 3254 Chinese reservoirs

Youjiang Shen et al., Earth System Science Data, <https://doi.org/10.5194/essd-15-2781-2023>

1. Summary of CaMa-Flood development in 2022-2024

[G1] Recent model updates (Yamazaki)

We released **CaMa-Flood v4** in March 2021. This is a major version update of CaMa-Flood which contains (1) refactoring of the source code structure for more flexibility use and (2) upgrade of the baseline topography data using MERIT DEM and MERIT Hydro.

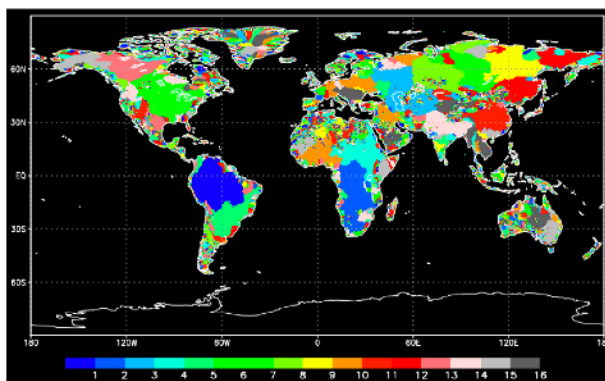
Since the release of CaMa-Flood v4, several moderate updates have been released.

1. CaMa-Flood v4.1 (released in January 2023)

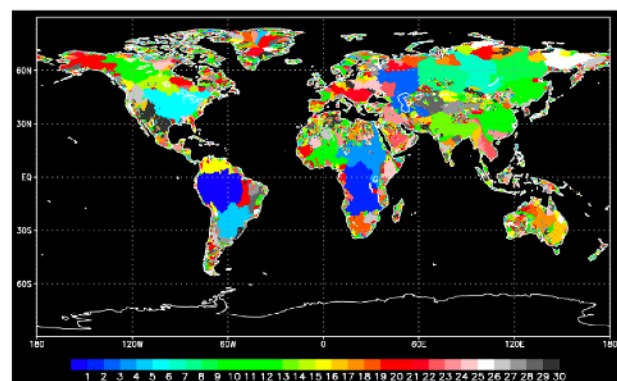
<Model Speedup> This update is primary for the improvement of computational efficiency. The single precision mode was implemented, which makes the simulation speed almost double compared to the previous simulation using double precision variables without degrading simulation accuracy.

In addition, hybrid parallelization using both MPI and OpenMP was activated, which is designed for the use of CaMa-Flood on supercomputers or cluster machines. The model grids are grouped following the river basin boundaries, and allocated to MPI nodes while minimizing the needs for data communication between MPI nodes. In default, parallelization up to 16 MPI nodes are available. If some minor inter-basin connection channels are neglected, parallelization up to 30 MPI nodes is possible. By combining MPI parallelization with OpenMP, more CPU can be used for faster simulation

We also prepare a documentation focusing on CaMa-Flood's computational efficiency, which is included in doc/ directory. Please refer to the file: [Note_HighPerformanceComputing.docx](#)



MPI_proc=16 @15min



MPI_proc=30 (size thrs=3%) @15min

2. CaMa-Flood v4.2 (released in April 2024)

<Reservoir Operation>

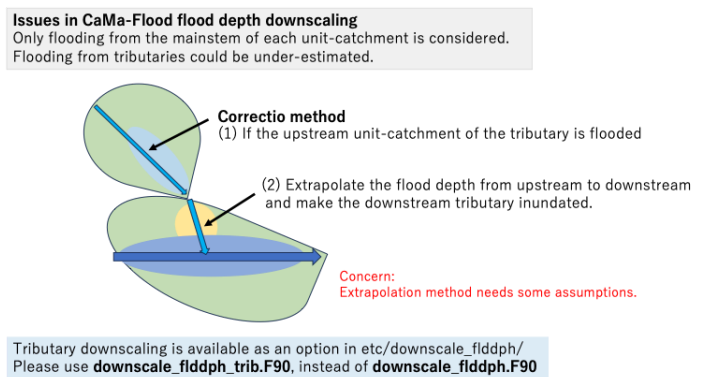
An improved reservoir operation scheme was implemented, and now reservoir operation can be used as a default option. We solved several issues in the previous reservoir operation formulations, and proposed a more stable scheme. Description of the new scheme is available in [Funato et al., in review].

<https://doi.org/10.22541/essoar.172978618.83964712/v1>

The manual for using reservoir operation scheme is prepared and available in doc/ directory. Please read: [Manual_ReservoirOperation_v420.docx](#)

<Better Downscaling Method>

A new downscaling method considering the flooding in the secondary channel in each unit-catchment is developed. This downscaling assumes linear-interpolation of flood depth between the upstream catchment and downstream catchment. This interpolation helpful for representing secondary channel inundation (yellow color in right figure), while this might introduce some uncertainties.



The detail is explained in the manual in doc/ directory: [Note_Downscaling.docx](#)

3. Ongoing updates for the next version (v4.3)

Some developments are ongoing for the next version. (1) A primitive version of levee protection scheme is currently being tested (Zhao et al., in review, <https://doi.org/10.22541/essoar.173758251.14316524/v1>). (2) A tracer scheme which can be used for analysis of material flow along river network is being developed.

4. GitHub code management

The CaMa-Flood source code is managed on GitHub. If you have developed a new scheme or fixed a bug, please contact the primary developer Dai Yamazaki for integrating your development to the master branch. https://github.com/global-hydrodynamics/CaMa-Flood_v4

[G2] Model skill improvement (Xudong)

We have developed a Benchmarking System designed to comprehensively evaluate the performance of the CaMa-Flood model. While its primary focus is on CaMa-Flood, the system is also extendable for evaluating various model settings, enabling users to assess improvements or deteriorations resulting from model modifications. By incorporating necessary pre-processing methods, the system facilitates comparisons between CaMa-Flood and other models, even those with different structures. As a result, this benchmarking system serves as an easy-to-use and valuable tool for future developments in CaMa-Flood and the broader river modeling community.

Key Features of the Benchmarking System:

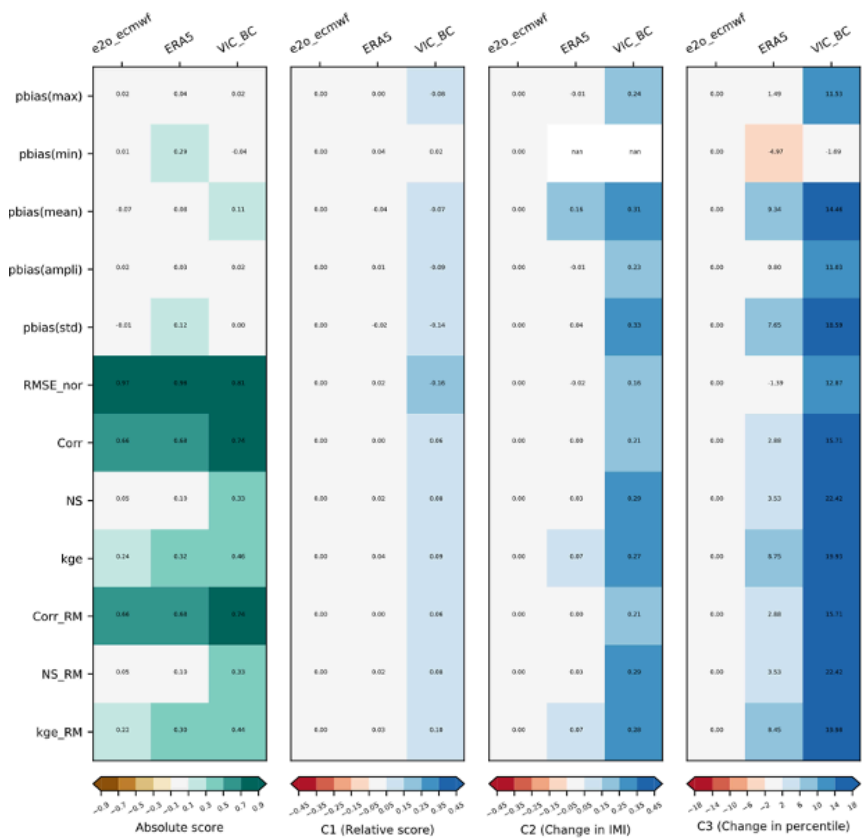
- 1. Integration of Various Observations:** The system combines remote sensing data (e.g., river water surface elevation, water surface area) with traditional in-situ observations (e.g., river discharge). This allows for the evaluation of model performance in estimating dynamic variables beyond river discharge, which vary significantly in space. Additionally, it expands the geographical coverage of model evaluation, particularly in data-scarce regions such as Asia and Africa.
- 2. Comprehensive Evaluation Metrics:** The system incorporates a wide range of evaluation indices (e.g., bias, correlation, Nash-Sutcliffe Efficiency, Kling-Gupta Efficiency) to capture different aspects of model performance. This enables a holistic assessment of model capabilities, covering both state and process evaluations.
- 3. Advanced Comparing Strategies:** The system introduces a percentile index for fair and consistent comparisons across different metrics and variables, alongside two other traditional comparison strategies. It also employs grouping strategies to categorize and compare model performance based on specific criteria (e.g., regions, river sizes, climate zones).
- 4. Visualization Tools:** Built-in visualization styles, including point maps and heatmaps, are provided to display spatial variations in model performance and highlight areas of improvement or deterioration. These tools enable easy interpretation of evaluation results and comparison metrics.
- 5. Ease of Use:** The benchmarking system is designed for easy execution with a simple command-line interface. It also allows users to customize and extend the system, such as adding new evaluation metrics or modifying visualization styles.

Conclusion: The benchmarking system offers a standardized and flexible framework for evaluating global river models. By integrating diverse observations, employing comprehensive evaluation metrics, and providing advanced comparison and visualization tools, the system supports both model development and intercomparison efforts. Its user-friendly design ensures broad applicability and adaptability for

future enhancements, benefiting both internal CaMa-Flood users and the wider river modeling community.

Recent Developments: This year, we published the paper "Benchmark Framework for Global River Models" in the Journal of Advances in Modeling Earth Systems. The benchmarking system was applied to simulations driven by various runoff inputs, including ERA5, earth2observe, and VIC-BiasCorrected (VIC-BC). The results demonstrate that model outputs driven by VIC-BC runoff outperform the others, as VIC-BC has been rigorously verified and calibrated. While modeled river discharge shows an acceptable level of agreement with observations, the performance of WSE and WSA requires further improvement. This may be due to limitations in model physics in capturing local dynamics or inaccuracies in satellite observations caused by technological constraints. Therefore, we encourage users, particularly internal users, to utilize VIC-BC as the runoff input when it aligns with their simulation purposes.

Figure. The overall performance of different models (a) and their comparison (b,c,d) regarding river discharge. a. the median value of different metrics among all river discharge gauges. b,c, and d shows the changes in the metrics of the new model (m1,m2) compared to the benchmark m0, representing the (b) relative score, (c) change in IMI and (d) change in percentile, respectively. The colors represent whether the improvement (in blue) or deterioration (in red) is significant.



Future Plans: Starting next year, we plan to regularly evaluate accuracy improvements at the end of each year. The benchmarking system results will also serve as a supporting tool for any future model updates. We welcome collaborations to further enhance the benchmarking system and its applications.

2. CaMa-Flood achievement reports.

2A: CaMa-Flood milestone papers before 2021

List of milestone achievements in before 2021

[A1] Global Flood Risk under Climate Change

Global exposure to flooding from the new CMIP6 climate model projections

Yukiko Hirabayashi, et al. 2013, Nature Climate Change, <https://doi.org/10.1038/nclimate1911>

Yukiko Hirabayashi, et al. 2021, Scientific Reports, <https://doi.org/10.1038/s41598-021-83279-w>

[A2] The critical role of the routing scheme in simulating peak river discharge in global hydrological models

Local floods induce large-scale abrupt failures of road networks

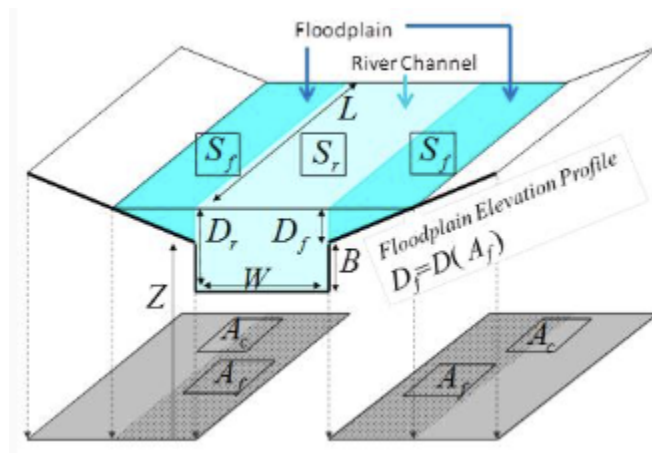
Fang Zhao, et al. 2017, Environmental Research Letters, <https://doi.org/10.1088/1748-9326/aa7250>

[A3] Local floods induce large-scale abrupt failures of road networks

Weiping Wang et al., 2019, Nature Communications, <https://doi.org/10.1038/s41467-019-10063-w>

[A4] Role of dams in reducing global flood exposure under climate change

Julien Boulange et al., 2021, Nature Communications , <https://doi.org/10.1038/s41467-020-20704-0>





[A1] Global Flood Risk under Climate Change

Global exposure to flooding from the new CMIP6 climate model projections

Yukiko Hirabayashi, Masahiro Tanoue, Orié Sasaki, Xudong Zhou, and Dai Yamazaki
(Shibaura Institute of Technology/The University of Tokyo)

Nature Climate Change, 2013, <https://www.nature.com/articles/nclimate1911>

Scientific Reports, 2021, <https://www.nature.com/articles/s41598-021-83279-w>

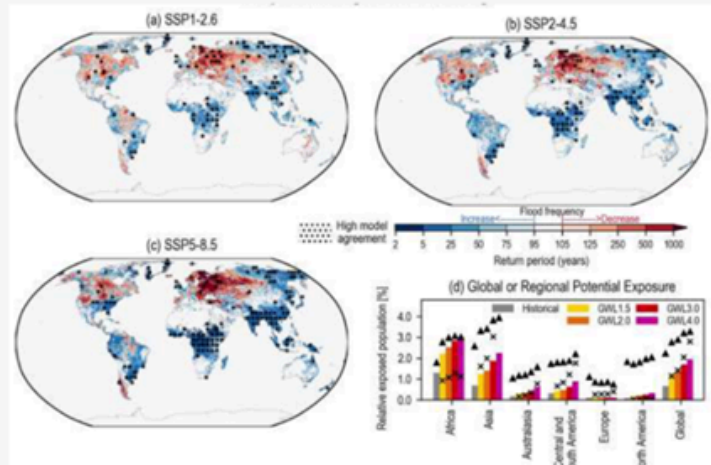
Nature Climate Change, 2021, <https://www.nature.com/articles/s41558-021-01158-8>

Scientific Reports, 2022, <https://www.nature.com/articles/s41598-022-25182-6>

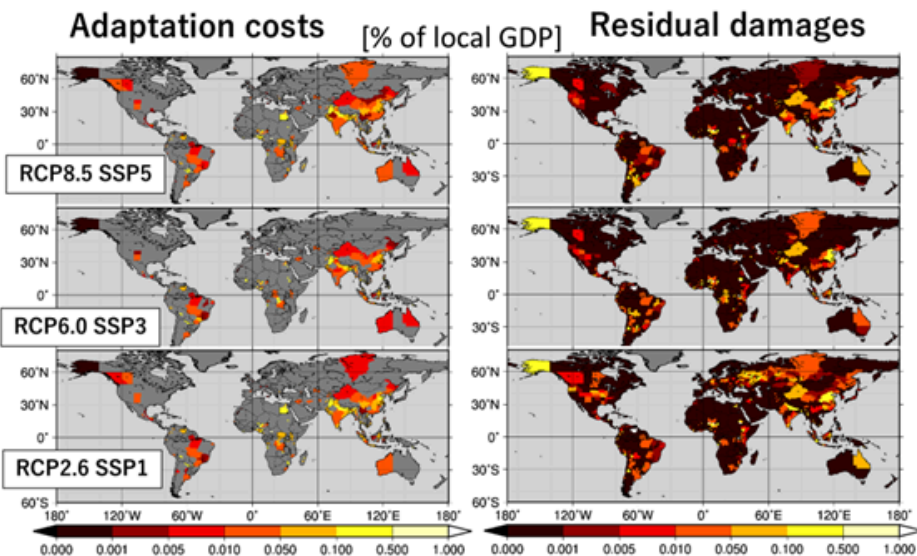
Abstract: Anthropogenic climate change has led to changes in the global water cycle, resulting in more intense precipitation and associated floods. Global inundation calculations from CaMa-Flood, with bias correction and downscaling, enable us to estimate the impact of flood risk in both the past and future, as well as the required adaptation measures and residual flood damage (RFD). The cost-benefit analysis of adaptation measures in future climates shows that China, India, and Latin American countries can achieve higher levels of flood protection, which will reduce RFD even under extreme scenarios. However, a high RFD (exceeding 0.1% of subnational administrative gross domestic product) remains, particularly in eastern China, northern India, and central Africa. RFD could be reduced with shorter construction periods or lower adaptation costs. Moreover, large ensemble climate experiments demonstrate that human-induced climate change has increased the probability of flood occurrences in these regions, with these changes becoming more pronounced in recent years. This highlights the need for immediate and appropriate adaptation actions, including enhanced financial support for high-risk regions.

Projected changes in floods

- Estimated increase in population affected by river flooding is 120% for 2°C and 400% for 4°C warming.
- The highest numbers of people affected by river flooding are projected for counties in southern, eastern and south-eastern Asia.



Adaptation Costs and residual damages of river flooding



- China, India and Latin American countries can achieve higher levels of flood protection that will reduce RFD even under extreme scenarios.
- However, a high RFD (exceeding 0.1% of local GDP) remains, especially in eastern China, northern India and central Africa.

Tanoue et al (2021),
Nature Climate Change

[A2] The critical role of the routing scheme in simulating peak river discharge in global hydrological models

Fang Zhao, T.I.E. Veldkamp, Katja Frieler, Jacob Schewe, Sebastian Ostberg, Sven Willner, Bernhard Schaubberger, Simon Gosling, H. Müller Schmied, F.T. Portmann, G. Leng, M. Huang, X. Liu, Q. Tang, N. Hanasaki, H. Biemans, D. Gerten, Y. Satoh, Y. Pokhrel, T. Stacke, P. Ciais, J. Chang, A. Ducharne, M. Guimberteau, Y. Wada, H. Kim, D. Yamazaki

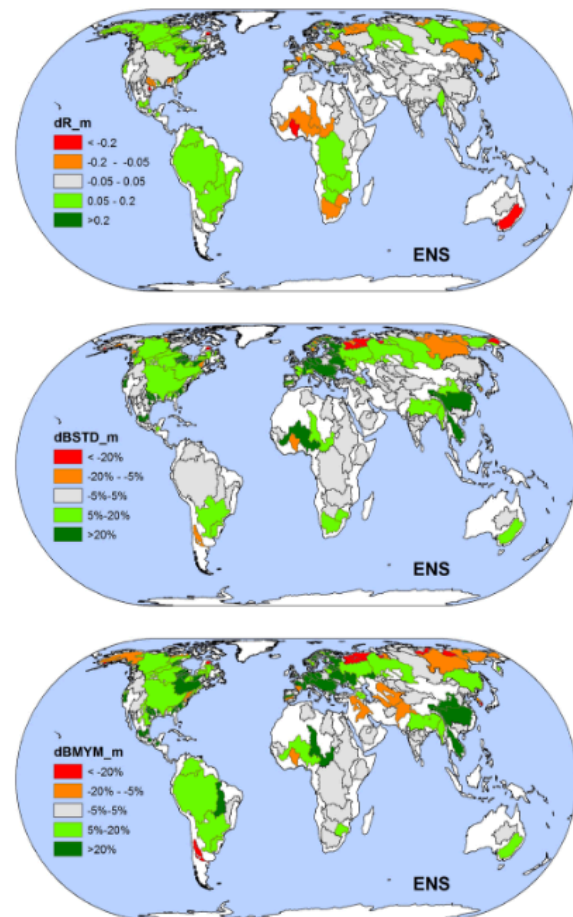
Potsdam Institute for Climate Impact Research, Potsdam, Germany
(current affiliation: East China Normal University)

Environmental Research Letters, <https://doi.org/10.1088/1748-9326/aa7250>

Abstract: Global hydrological models (GHMs) have been applied to assess global flood hazards, but their capacity to capture the timing and amplitude of peak river discharge—which is crucial in flood simulations—has traditionally not been the focus of examination. Here we evaluate to what degree the choice of river routing scheme affects simulations of peak discharge and may help to provide better agreement with observations. To this end we use runoff and discharge simulations of nine GHMs forced by observational climate data (1971–2010) within the ISIMIP2a project. The runoff simulations were used as input for the global river routing model CaMa-Flood. The simulated daily discharge was compared to the discharge generated by each GHM using its native river routing scheme. For each GHM both versions of simulated discharge were compared to monthly and daily discharge observations from 1701 GRDC stations as a benchmark. CaMa-Flood routing shows a general reduction of peak river discharge and a delay of about two to three weeks in its occurrence, likely induced by the buffering capacity of floodplain reservoirs. For a majority of river basins, discharge produced by CaMa-Flood resulted in a better agreement with observations. In particular, maximum daily discharge was adjusted, with a multi-model averaged reduction in bias over about 2/3 of the analysed basin area. The increase in agreement was obtained in both managed and near-natural basins. Overall, this study demonstrates the importance of routing scheme choice in peak discharge simulation, where CaMa-Flood routing accounts for floodplain storage and backwater effects that are not represented in most GHMs. Our study provides important hints that an explicit parameterisation of these processes may be essential in future impact studies.

Introduction: Fluvial flooding is a major hazard that is expected to worsen with climate change—especially in Asia and Africa. Yet, global hydrological models often struggle to simulate peak discharge because of coarse resolution, uncertain precipitation inputs, and oversimplified processes. Their river routing schemes typically overlook floodplain storage and backwater effects. The CaMa-Flood model, using a diffusive wave equation and high-resolution topography, explicitly resolves these dynamics. However, its performance relative to native routing schemes in global models remains untested.

Results: When forced with daily runoff from nine GHMs, CaMa-Flood’s explicit treatment of floodplain processes delayed the daily peak by about 18 days and reduced maximum discharge by 22% compared to the models’ native routing schemes. This delay did not always improve timing correlation, but performance metrics related to peak flows (e.g., annual maximum biases) improved significantly over 63% of the global basin area examined, notably in Southeast and East Asia, Eastern Europe, and parts of Tropical Africa and South America. In basins already featuring wetland or floodplain representations (e.g., in MPI-HM and ORCHIDEE), CaMa-Flood showed less added benefit, and a small number of basins in Central and West Asia and Eastern Siberia displayed worse performance. Overall, the inclusion of floodplain storage and backwater effects in CaMa-Flood accounted for much of the reduction in peak-flow overestimation in GHMs lacking these processes, thereby narrowing inter-model variability in peak discharge simulations.



Conclusion: CaMa-Flood delayed and reduced peak discharge compared to most GHM routing schemes, improving performance both in near-natural and managed basins. These gains likely stem from its explicit floodplain representation, the buffering capacity of which smooths hydrographs and reduces inter-model differences. Our results highlight the critical role of routing schemes in peak discharge simulations.



[A3] Local floods induce large-scale abrupt failures of road networks

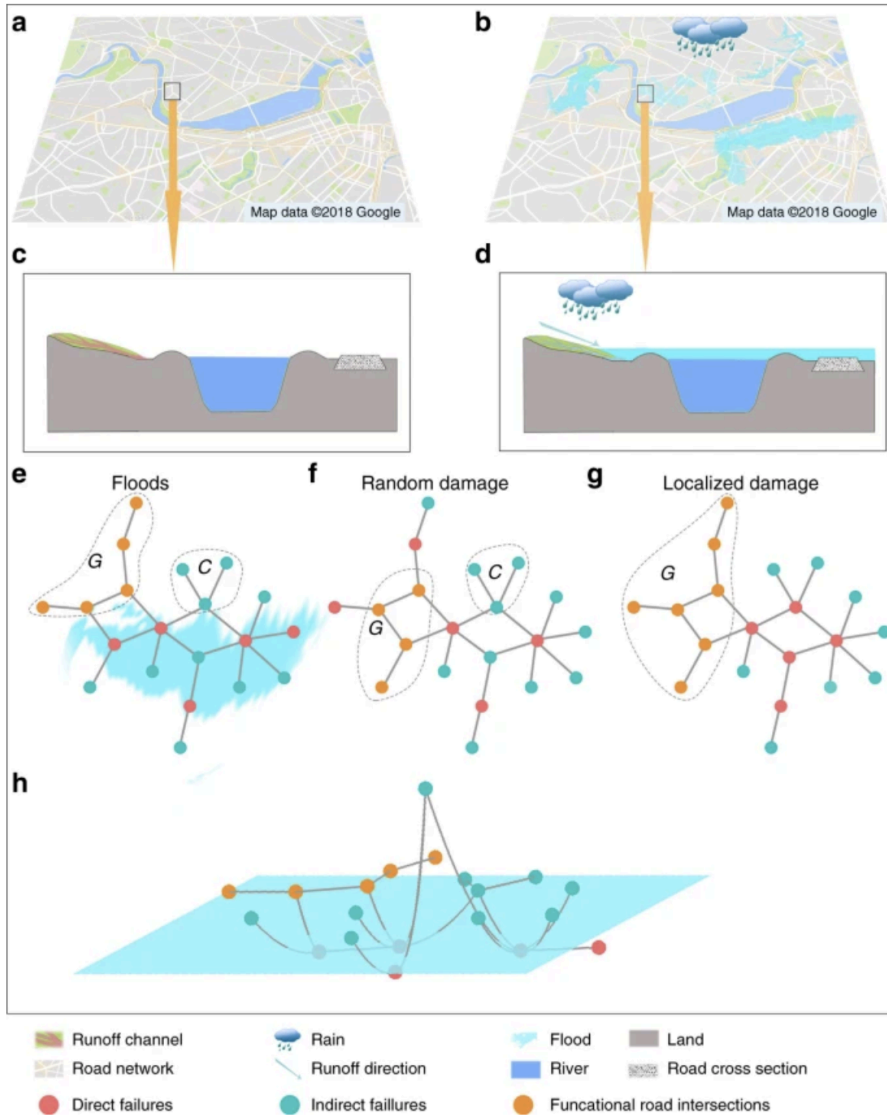
Weiping Wang et al., 2019, Nature Communications, <https://doi.org/10.1038/s41467-019-10063-w>

State Key Laboratory of Earth Surface Processes and Resource Ecology, Beijing Normal University, Beijing

Abstract:

The adverse effect of climate change continues to expand, and the risks of flooding are increasing. Despite advances in network science and risk analysis, we lack a systematic mathematical framework for road network percolation under the disturbance of flooding. The difficulty is rooted in the unique three-dimensional nature of a flood, where altitude plays a critical role as the third dimension, and the current network-based framework is unsuitable for it. Here we develop a failure model to study the effect of floods on road networks; the result covers 90.6% of road closures and 94.1% of flooded streets resulting from Hurricane Harvey. We study the effects of floods on road networks in China and the United States, showing a discontinuous phase transition, indicating that a small local disturbance may lead to a large-scale systematic malfunction of the entire road network at a critical point. Our integrated approach opens avenues for understanding the resilience of critical infrastructure networks against floods.

Fig. 1



Schematic diagram of floods and demonstration of the effects of floods, random damage, and localized damage on a road system. a River and road network without flooding. b River and road network when rainfall-induced flooding inundates some road segments. c Sectional view of the boxed region in a. d Sectional view of the boxed region in b. The rainfall forms runoff on the ground. A large amount of runoff converges into a flood and inundates some road segments. The flood follows the river channel and damages infrastructure (e.g., roads) in a river basin. The flood-induced failures have a distinct trajectory. Schematic demonstrations of (e) random damage and (g) localized damage in a sketched network respectively. f 2D and h 3D views of flood disturbance in the sketched network

[A4] Role of dams in reducing global flood exposure under climate change

Julien Boulange et al., 2021, Nature Communications , <https://doi.org/10.1038/s41467-020-20704-0>

Abstract: Globally, flood risk is projected to increase in the future due to climate change and population growth. Here, we quantify the role of dams in flood mitigation, previously unaccounted for in global flood studies, by simulating the floodplain dynamics and flow regulation by dams. We show that, ignoring flow regulation by dams, the average number of people exposed to flooding below dams amounted to 9.1 and 15.3 million per year, by the end of the 21st century (holding population constant), for the representative concentration pathway (RCP) 2.6 and 6.0, respectively (Fig. 1). Accounting for dams reduces the number of people exposed to floods by 20.6 and 12.9% (for RCP2.6 and RCP6.0, respectively). While environmental problems caused by dams warrant further investigations, our results indicate that consideration of dams significantly affect the estimation of future population exposure to flood, emphasizing the need to integrate them in model-based impact analysis of climate change.

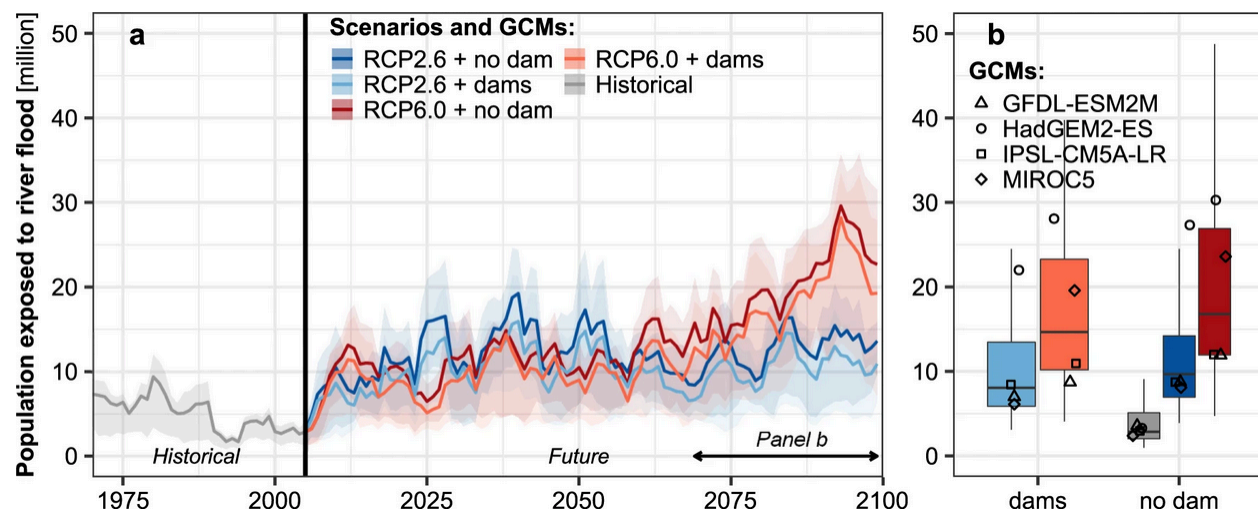


Fig. 1: Population exposure to the historical 100-year river flood (keeping population constant at 2010 level) downstream of dams. **a** 5-year moving averages of the population living below dams exposed to the historical 100-year river flood for historical (grey line) and future simulations for 2 RCPs and experiments (colour lines). The uncertainty range represents the spread among GCMs. **b** The 95th and 5th range (whiskers), median (horizontal lines in each bar), and 1st and 3rd quartiles (height of box) and individual mean values among GCMs (markers) of the population exposed to the historical 100-year flood for grid-cells located below dams over the 2070–2099 period.

2B: Papers/achievements on CaMa-Flood development

List of papers on CaMa-Flood development in 2022-2024

[B1] Assimilation of transformed water surface elevation to improve river discharge estimation in a continental-scale river

Menaka Revel, et al. 2023, Hydrology & Earth System Sciences, <https://doi.org/10.5194/hess-27-647-2023>

[B2] A globally applicable framework for compound flood hazard modeling

Dirk Eilander et al., Natural Hazard & Earth System Sciences, <https://doi.org/10.5194/nhess-23-823-2023>

[B3] Inundation prediction in tropical wetlands from JULES-CaMa-Flood global land surface simulations

Toby Marthews et al., Hydrology and Earth System Sciences, 2022, <http://doi.org/10.5194/hess-26-3151-2022>

[B4] A New Generation of Hydrological Condition Simulator Employing Physical Models and Satellite-based Meteorological Data

Wenchao Ma et al., Earth and Space Science, 2024, <https://doi.org/10.1029/2023EA003228>

[B5] Multivariable Integrated Evaluation of Hydrodynamic Modeling: A Comparison of Performance Considering Different Baseline Topography Data

Prakat Modi et al., Water Resources Research, 2022, <https://doi.org/10.1029/2021WR031819>

[B6] Correction of River Bathymetry Parameters Using the Stage–Discharge Rating Curve

Xudong Zhou et al. 2022, Water Resources Research, <https://doi.org/10.1029/2021WR031226>

[B1] Assimilation of transformed water surface elevation to improve river discharge estimation in a continental-scale river

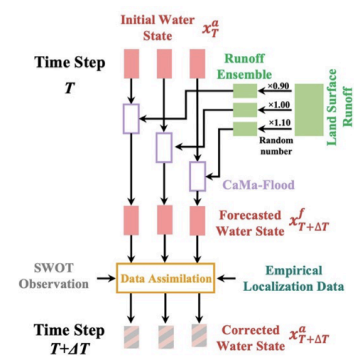
Menaka Revel, Xudong Zhou, Dai Yamazaki, and Shinjiro Kanae

University of Waterloo, Canada / Institute of Industrial Science, UTokyo, Japan

Hydrology and Earth System Sciences, 2023, <https://doi.org/10.5194/hess-27-647-2023>

Abstract: Hydrodynamic modeling is an important instrument for understanding water resources and managing associated risks. However, the complexity of hydrological systems and limited reliable data present challenges to accurately simulating surface water dynamics. Data assimilation techniques address these issues by integrating observations into hydrological models, enhancing precision, and reducing uncertainty. The CaMa-Flood Data Assimilation (CaMa DA) system is a framework designed for assimilating satellite data into the CaMa-Flood hydrodynamic model. The workflow includes preparing physically based adaptive empirical localization parameters, generating runoff perturbations, pre-processing observations, and performing data assimilation. Localization parameter preparation involves standardizing simulations, deriving patches using semi-variogram analysis, and calculating parameters. Runoff perturbations are generated using simple, normal, or lognormal methods. Observations, such as satellite altimetry, require pre-processing to align observation locations with the river network. The system supports various data assimilation methods, including direct, anomaly, normalized value, and log-transformed value assimilations. Leveraging the computational efficiency of the CaMa-Flood model and adaptive empirical localization, the system is well-suited for global-scale applications. Despite model limitations, normalized value assimilation has shown strong performance in natural river systems like the Amazon basin, while anomaly assimilation is more effective in human-altered basins like the Mississippi. With upcoming satellite missions such as SWOT and NISAR, the CaMa-DA framework promises to advance our understanding of surface water dynamics.

Introduction: Monitoring global river hydrodynamics is essential for understanding the Earth's hydrological cycle, the climate system, and mitigating water-related hazards such as floods and droughts. With the 2020s being regarded as the “Golden Era” of satellite remote sensing for surface waters, an unprecedented opportunity has emerged to integrate satellite-derived observations into global river models. To capitalize on this, we developed a novel data assimilation framework that incorporates satellite observations into the CaMa-Flood hydrodynamic model. Designed with the upcoming Surface Water and Ocean Topography (SWOT) Mission in mind, this framework enables accurate estimation of river discharge on a global scale while maintaining low computational costs. A key feature of



the framework is its physically based, adaptive, empirical localization method, which optimizes the use of satellite observations for hydrodynamic modeling. This innovative approach represents a significant advancement in global-scale river modeling, offering transformative potential for improving our understanding and management of river systems worldwide.

Methods: The CaMa-Flood Data Assimilation (CaMa-DA) system, designed to assimilate satellite data into the CaMa-Flood hydrodynamic model, includes workflows such as preparing adaptive empirical localization parameters, generating runoff perturbations using normal or lognormal methods, pre-processing satellite altimetry data to align with river networks, and performing data assimilation (DA) through various methods, including direct, anomaly, normalized value, and log-transformed value assimilation, ensuring robust and flexible performance across diverse hydrodynamic conditions. Expansion of the assimilation domain to maximize observations is limited by error covariance caused by limited ensemble size in complex river networks. Therefore, we developed a physically based empirical localization method to maximize the observations available while filtering error covariance areas. Physically based empirical local patches were derived separately for each river pixel, considering spatial autocorrelations (Revel et al., 2019). Moreover, we developed an automated altimetry mapping procedure (AltiMaP) that allocates satellite altimetry Virtual Stations to the MERIT Hydro considering the braided and non-braided rivers, land, river, and ocean classifications (Revel et al., 2024). We further investigated the potential of direct, anomaly, and normalized value DA methods to improve river discharge estimates under the current limitations of hydrodynamic modeling.

Results: Assimilation works well in large rivers especially in downstream, because upstream discharge is corrected frequently (Revel et al., 2021). Normalized value assimilation demonstrated the best performance among the tested methods, improving river discharge estimates for 62% of stream gauges and significantly enhancing water surface elevation (WSE) variations, particularly under the limitations of hydrodynamic models. Despite challenges such as parameter uncertainties and model simplifications, it consistently outperformed direct and anomaly DA methods, achieving high accuracy with Nash–Sutcliffe efficiency (NSE) values exceeding 0.6 in most cases and notable improvements in the Amazon basin (Revel et al., 2023).

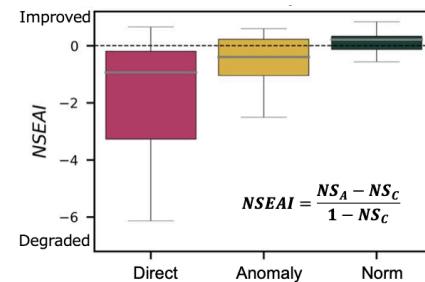


Figure 2: Boxplot of NSE-based assimilation index⁴⁴

Conclusions: Utilizing the computationally efficient CaMa-Flood model in conjunction with an advanced DA approach, we successfully developed a global-scale data assimilation system, referred to as the CaMa-DA system. The primary components of this system include: (1) the generation of empirical local patches, (2) the mapping of satellite altimetry observations to model river grids, and (3) the implementation of an assimilation methodology that accounts for bias correction. Future challenges include evaluating the quality of the assimilated discharge products and addressing model biases to enhance the robustness and accuracy of DA estimates.

[B2] A globally applicable framework for compound flood hazard modeling

Dirk Eilander et al., Natural Hazard & Earth System Sciences, <https://doi.org/10.5194/nhess-23-823-2023>

Abstract: Coastal river deltas are prone to flooding from pluvial, fluvial, and coastal drivers. Compound floods, resulting from these drivers' co-occurrence, may worsen impacts compared to single-driver floods. Existing global flood models overlook compound flooding, while local models are hard to scale to new locations. We therefore developed a globally applicable framework for compound flood hazard modeling, using 2D hydrodynamic SFINCS model setup based on global datasets, and coupled to the CaMa-Flood river routing model, and Global Tide and Surge Model. The goal of this study is to present the framework, to test its ability to simulate compound floods in data-sparse coastal deltas, and to demonstrate how it can be used for compound flood analysis. Testing with Tropical Cyclones Idai and Eloise in Mozambique, our model outperforms the global CaMa-Flood model for compound flooding, offering more realistic flood depth maps. Furthermore, we show it can be used to determine the dominant flood drivers and transition zones between flood drivers. We argue that a wide range of plausible events should be investigated to obtain a robust understanding of compound flood interactions, which is important to understand for flood adaptation, preparedness, and response.

Methods: The globally applicable compound flood hazard framework is shown in Fig. 1. The tide and surge components are simulated with the Global Tide and Surge Model (GTSM) version 3.0. The model is forced with mean sea level pressure and 10m wind components from ERA5 merged with wind and pressure fields from the Holland parametric wind model based on IBTrACS data for the tropical cyclones. Riverine discharge is simulated with the global river routing modeling CaMa-Flood version 4.0.1 including its bifurcation scheme. The model is forced with ERA5 runoff. The hydrodynamic SFINCS model is automatically built based on global datasets, facilitated by HydroMT v0.4.5, a Python package for automated model building. The approach is modular as datasets can easily be interchanged and many workflows to process raw data into model input data can be reused for different models. High-resolution (10m) flood extent data are derived from Sentinel-1 synthetic aperture radar (SAR) images and used to compute the model skill.

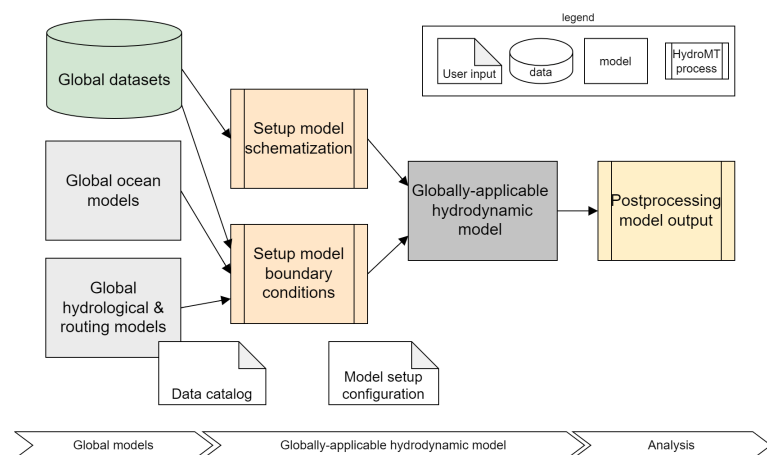


Fig. 1: Framework for globally applicable compound flood modelling

Results: Compared to the global CaMa-Flood model, the globally applicable SFINCS model generally performs better in terms of the critical success index (−0.01–0.09) and hit rate (0.11–0.22) but worse in terms of the false-alarm ratio (0.04–0.14), see Fig 2. Furthermore, the simulated flood depth maps are more realistic due to better floodplain connectivity and they provide a more comprehensive picture as direct coastal flooding and pluvial flooding are simulated. Using the new framework, we determine the dominant flood drivers and transition zones between flood drivers. These vary significantly between both events because of differences in the magnitude of and time lag between the flood drivers.

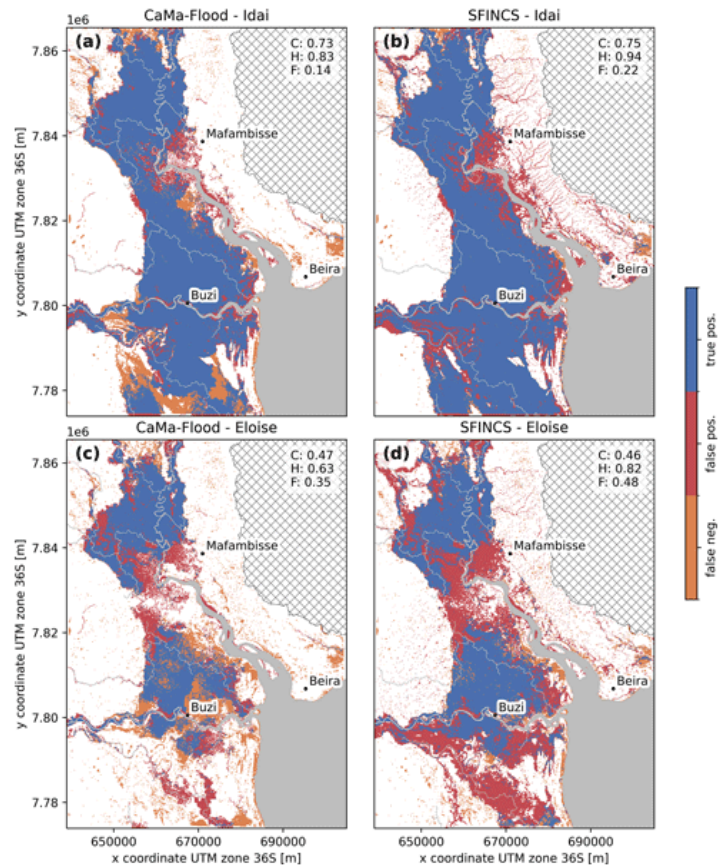


Fig. 2: Skill of the maximum flood extents of CaMa-Flood (left) and SFINCS (right) for tropical cyclone Idai (top) and Eloise (bottom)

Conclusions: Here, we presented an automated framework to model compound flooding anywhere on the globe in a reproducible and transparent manner, and we evaluated its suitability and use for identifying compound flood drivers. Compared to CaMa-Flood, the globally applicable SFINCS model can accommodate for direct coastal and pluvial flooding as well as interactions between coastal, pluvial, and fluvial drivers, thereby providing a more comprehensive description of flooding in coastal deltas. Furthermore, while the CaMa-Flood bifurcation scheme largely improves the results, the floodplain connectivity is still limited, resulting in higher flood levels and smaller flood extents. However, pluvial flooding is likely overestimated in the globally applicable SFINCS model as small streams are not represented in the model, thus underestimating the drainage capacity. Finally, we found that the transition zones between flood drivers vary significantly between flood events due to differences in the relative timing between and magnitude of each driver.

[B3] Inundation prediction in tropical wetlands from JULES-CaMa-Flood global land surface simulations

Toby R. Marthews, Dadson SJ, Clark DB, Blyth EM, Hayman G, Yamazaki D, Becher ORE, Martínez-de la Torre A, Prigent C & Jiménez C

(UK Centre for Ecology & Hydrology and partner institutions)

Environmental Research Letters, 2023, <https://hess.copernicus.org/articles/26/3151/2022/>

Abstract: Wetlands play a key role in hydrological and biogeochemical cycles and provide multiple ecosystem services to society. However, reliable data on the extent of global inundated areas and the magnitude of their contribution to local hydrological dynamics remain surprisingly uncertain. Global hydrological models and Land Surface Models (LSMs) include only the most major inundation sources and mechanisms, therefore quantifying the uncertainties in available data sources remains a challenge. We address these problems by taking a leading global data product on inundation extents (Global Inundation Extent from Multi-Satellites, GIEMS) and matching against predictions from a global hydrodynamic model (CaMa-Flood) driven by runoff data generated by a land surface model (Joint UK Land and Environment Simulator, JULES). The ability of the model to reproduce patterns and dynamics showed by the observational product is assessed in a number of case studies across the tropics, which show that it performs well in large wetland regions, with a good match between corresponding seasonal cycles. At finer spatial scale, we found that water inputs (e.g. groundwater inflow to wetland) became underestimated in comparison to water outputs (e.g. infiltration and evaporation from wetland) in some wetlands (e.g. Sudd, Tonlé Sap) and the opposite occurred in others (e.g. Okavango) in our model predictions. We also found evidence for an underestimation of low levels of inundation in our satellite-based inundation data (approx. 10% of total inundation may not be recorded). Additionally, some wetlands display a clear spatial displacement between observed and simulated inundation as a result of over- or under-estimation of overbank flooding upstream. This study provides timely information on inherent biases in inundation prediction and observation that can contribute to our current ability to make critical predictions of inundation events at both regional and global levels.

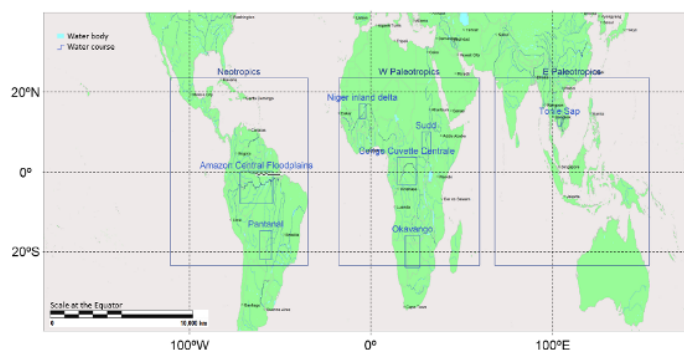


Figure 1: Tropical wetlands and inundated areas referred to in this study.

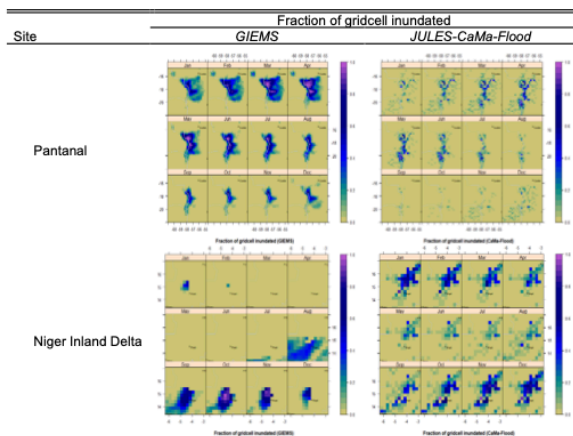


Figure 3: Fraction of gridcell inundated (in addition to water contained in channels and watercourses, which are not shown) for our first two study areas. Data shown are an average for 1992-2014 from *GIEMS-2* observations (left) and equivalent *JULES-CaMa-Flood* simulations (right).

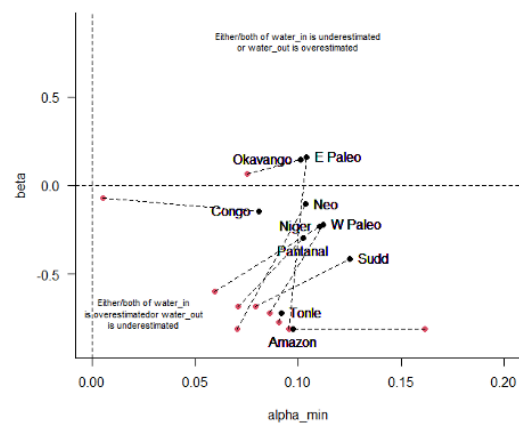


Figure 7: Optimal values of β and α_{min} , calculated as the centroids of the maximal region on the KGE plots (black) or NSE plots (red) for each site (with $\alpha_{max}=1.0$). On this plot, we define $water_{in} = (\text{channel} + \text{surface} + \text{subsurface inflow} + \text{precipitation})$ and $water_{out} = (\text{infiltration} + \text{evaporation})$.

Conclusions: Simulations of inundation extent are important because they allow us to predict what will happen to globally-important wetlands in the future. Wetlands are known to be key nodes in the biosphere system in terms of vulnerability to climate change. However, wetlands are also highly dynamic landscape-level entities produced by the balance of a number of different water cycle processes acting together, not all of which are yet represented in global hydrodynamic models.

Reducing uncertainty in predictions from large-scale inundation models has long been a prerequisite for their use in global Earth system models. In this study we have shown that a very reasonable and close match may be derived between *JULES-CaMa-Flood* model predictions of inundation extent and independent *GIEMS-2* global satellite-based observations of inundation. Differences do occur at regional scale in particular large wetlands, however, and these differences indicate clearly the importance of incorporating into the modelling framework a better representation of the hydrological impacts of, especially, infiltration, evaporation and groundwater-fed inundation. These comments are not only relevant to *GIEMS-2* and *JULES-CaMa-Flood* data: all satellite-based inundation data have biases that may be assumed to be very similar to those inherent in *GIEMS* data, and all model predictions of inundation have biases and uncertainties presumably similar to those that are in *JULES-CaMa-Flood* predictions, so we believe that our results and analysis provide a blueprint for users of other model/observational data on how they might assess and account for these types of bias in their own data.

Improving our understanding of the dynamics of inundated areas and the role they play in the generation of land-atmosphere fluxes requires a better representation in general of wetlands within global land-surface and hydrodynamic models. The results of this study point clearly towards the need for greater attention to be paid to hydrological dynamics and water cycle processes within these models, which we expect to result in improved modelling predictive capability in global wetlands in the future. A firm focus on producing a better characterisation of hydrodynamics within this class of models will produce enormous positive returns in terms of our global capability to predict inundation and its global impacts and will make a welcome contribution to our preparedness for the impacts of future climate change.

[B4] A New Generation of Hydrological Condition Simulator Employing Physical Models and Satellite-based Meteorological Data

Wenchao Ma, Kenshi Hibino, Kosuke Yamamoto, Haruya Yoshikawa, Kei Yoshimura

(Nanjing Normal University & Tokyo University & JAXA)

Earth and Space Science, 2024, <https://doi.org/10.1029/2023EA003228>

Abstract: Determining the distribution and dynamics of water on land at any given moment poses a significant challenge due to the constraints of observation. Consequently, as advancements in land surface models (LSMs) have been made, numerical simulation has emerged as an increasingly accurate and effective method for hydrological research. Nonetheless, systems that represent multiple land surface parameters in a near-real-time manner are scarce. In this study, we present an innovative land surface and river simulation system, termed Today's Earth (TE), which generates state and flux values for the near-surface environment with multiple outputs in near-real-time. There are currently three versions of TE, distinguished by the forcing data utilized: **JRA-55** version, employing the Japanese 55-year Reanalysis (JRA-55, from 1958 to the present); **GSMaP** version, utilizing the Global Satellite Mapping of Precipitation (GSMaP, from 2001 to the present); **MODIS** version, utilizing the Moderate Resolution Imaging Spectroradiometer (MODIS, from 2003 to the present). These long-term forcing datasets allow for outputs of the JRA-55 version from 1958, the GSMaP version from 2001, and the MODIS version from 2003. Aiming to provide water and energy values on a global scale in real-time, the TE system utilizes the LSM Minimal Advanced Treatments of Surface Interaction and Runoff (MATSIRO) (Takata et al., 2003, [https://doi.org/10.1016/s0921-8181\(03\)00030-4](https://doi.org/10.1016/s0921-8181(03)00030-4); Yamazaki et al., 2011, <https://doi.org/10.1029/2010wr009726>) at a horizontal resolution of 0.5° , along with the river routing model CaMa-Flood (Yamazaki et al., 2011, <https://doi.org/10.1029/2010wr009726>) at a horizontal resolution of 0.25° . Both land surface and river products are available in 3-hourly, daily, and monthly intervals across all three versions. A notable feature of TE is its ability to release both state and flux parameters in near-real-time, offering convenience for various aspects of hydrological research. In addition to presenting the general features of TE-Global, this study examines the performance of snow depth, soil moisture, and river discharge data in daily intervals from 2003 to 2021, with validation spanning 2003 to 2016. When comparing snow depth results, the correlation coefficient ranged between 0.644 and 0.658, while for soil moisture it ranged between 0.471 and 0.494. These findings suggest that the LSM yields comparable results when utilizing JRA-55, MODIS, or GSMaP. Interestingly, river output from the three products exhibited distinct characteristics varying from GSMaP to JRA-55 and MODIS. For river discharge, the correlation coefficient ranged from 0.494 to 0.519, the root mean square error ranged from $3,730 \text{ m}^3/\text{s}$ to $6,330 \text{ m}^3/\text{s}$, and the mean absolute error ranged from $3,000 \text{ m}^3/\text{s}$ to $5,160 \text{ m}^3/\text{s}$ among the different forcing versions. The overall bias in river discharge from GSMaP was $1,570 \text{ m}^3/\text{s}$, in contrast to $-589 \text{ m}^3/\text{s}$ for JRA-55 and $-200 \text{ m}^3/\text{s}$ for MODIS. These metrics demonstrate that the TE system is capable of generating practical land surface and river products, highlighting differences arising from the use of various types of forcing data. This comprehensive system would be valuable for monitoring water-related movements, predicting disasters, and contributing to sophisticated water resource management. Regarding its application, the TE system has been included in the World

Meteorological Organization as a Global Hydrological Modelling System. All TE-Global products can be freely accessed through File Transfer Protocol.

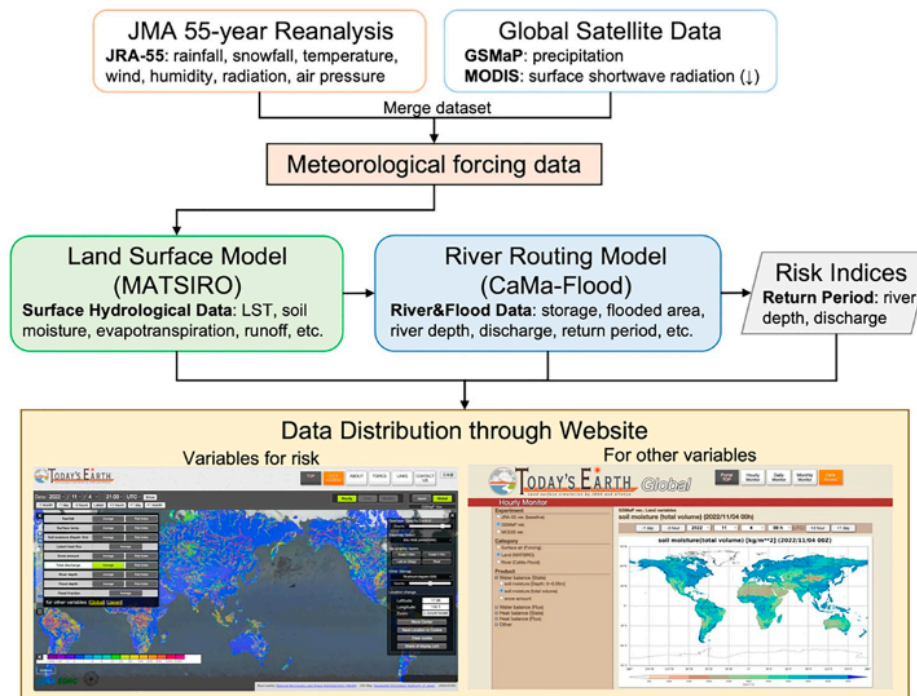


Figure1. Schematic figure for the TE-Global system (<https://www.eorc.jaxa.jp/water/>).

Conclusions: We present the validation results of the TE system, which simulates the global hydrological cycle on land areas using reanalysis meteorological data (JRA-55) and satellite-derived observation data (GSMaP, MODIS). We examined three variables (snow depth, soil moisture, and river discharge) to assess the performance of the system. Across all three versions, the TE system exhibited commendable performance, both spatially and temporally. In addition, seasonal variation was evident in the monthly average values. In the case of snow depth, all three versions exhibited similar patterns, with the JRA-55 version outperforming the others. Moreover, the simulation's advantages are evident in areas where observational techniques necessitate masking, thus offering a more exhaustive dataset without temporal and spatial gaps. Regarding river discharge, validation was somewhat constrained in this study. Nonetheless, various studies have demonstrated that CaMa-Flood is an efficacious approach for computing river discharge based on water surface slope and allows for computationally efficient simulations of global-scale river hydrodynamics (Hanazaki et al., 2022; Lu et al., 2016; Revel et al., 2021). Notably, the TE system can generate more than 60 variables in near-real-time.

It is important to note that biases and inadequacies in meteorological forcing data and models contribute to inaccuracies in TE system outputs. Regarding its application, the TE system has been included in the WMO as a Global Hydrological Modelling System. The TE group is committed to the ongoing enhancement of the system through model refinement, improvements in boundary conditions, resolution enhancement, and the effective utilization of satellite-derived observation data.

[B5] Multivariable Integrated Evaluation of Hydrodynamic Modeling: A Comparison of Performance Considering Different Baseline Topography Data

Prakat Modi, Menaka Revel, Dai Yamazaki

(Shibaura Institute of Technology, Japan/ University of Waterloo, Canada/ The University of Tokyo, Japan)

Water Resources Research, 2022, <https://doi.org/10.1029/2021WR031819>

Abstract: Continental-scale river hydrodynamic modeling helps to understand the global hydrological cycle, and model evaluation is essential for calibration and performance assessment. Although many models have been evaluated using several variables separately, methods for the integrated multivariable assessment have yet to be established. We proposed an integrated multivariable evaluation method and an overall basin skill score (OSK) metric, which integrates the sub-basin skill score, calculated by combining multiple variables' normalized Nash-Sutcliffe efficiency values. The sub-basin approach and OSK assess the model performance at the sub-basin and basin scales and overcome the observation-related limitations of different spatial dimensions. Evaluation of the CaMa-Flood global river model for the Amazon Basin considering three variables (discharge, water surface elevation, and flooded area) and two baseline topography data (Shuttle Radar Topography Mission (SRTM) and Multi-Error-Removed Improved-Terrain (MERIT) digital elevation models (DEMs)), shows that the proposed methodology can overcome the limitation of single-variable evaluation in identifying multiple best parameter sets due to low sensitivity. CaMa-Flood considering MERIT DEM achieves a single optimal parameter set with a maximum OSK of 0.57 compared with 0.52 for the SRTM DEM, and it shows the importance of accuracy of topography data for improvement in the performance of river hydrodynamic modeling. The proposed multivariable integrated evaluation with better topography data proved to help reduce equifinality and estimate the best parameter by maintaining the physical relationships among variables.

Introduction: Continental-scale river hydrodynamic modeling is crucial for understanding the global water cycle, flood monitoring, and water resource management. Digital elevation models (DEMs) are essential for representing topography, with accuracy being key to improving hydrodynamic model performance. However, evaluations of DEMs often focus on vertical accuracy rather than hydrodynamic performance. Hydrodynamic models are also affected by uncertainties in parameters like runoff and river bathymetry with traditional single-variable evaluations of hydrodynamic models often failing due to equifinality and misrepresentation of internal processes.

This study applies a multivariable integrated evaluation framework using the CaMa-Flood hydrodynamic model for the Amazon Basin to overcome the previous limitations. A new overall basin skill score (OSK) metric is proposed to objectively assess the model's performance across multiple variables with varying spatial and temporal dimensions. The study also evaluates the impact of topographic accuracy on hydrodynamic modeling by comparing the performance of MERIT and SRTM DEMs. This approach aims to enhance model accuracy, reduce equifinality, and provide a comprehensive assessment of river hydrodynamic simulations.

Methodology: We used the CaMa-Flood River hydrodynamic model to evaluate the performance of two Digital Elevation Models (DEMs) - SRTM and MERIT for the Amazon Basin. Simulations were conducted at a

0.1° resolution using runoff inputs and varying river depth and Manning's coefficient to consider the model uncertainties. The Amazon Basin was chosen for its complex river hydraulics and large seasonal floodplains. Observations of discharge (Q), water surface elevation (WSE), and flooded area (FA) were used as evaluation metrics. Daily discharge data for 418 locations, satellite-derived altimetry from ENVISAT, and the GIEMS-2 inundation dataset were compared to simulated results for accuracy. We used the subbasin approach to evaluate the model and integrate the metric score for various variables. Skill scores for sub-basins were computed for each DEM and parameter set using normalized Nash-Sutcliffe efficiency (NNSE). The overall model performance was assessed using a basin-wide skill score (OSK), combining all three variables. This approach facilitated multivariable integrated evaluation across sub-basins and basins, identifying the parameter set with maximum OSK for comparison of DEM performance.

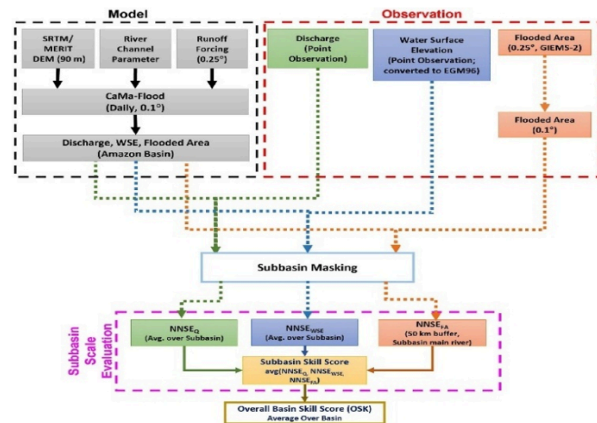


Figure 1: Study framework showing the flowchart of calculation of the overall basin skill score from sub-basin skill scores calculated using the normalized Nash-Sutcliffe efficiency

Results: We evaluated CaMa-Flood performance using the SRTM and MERIT DEMs for discharge (Q), water surface elevation (WSE), and flooded area (FA) using average NNSE values, separately. Single evaluation was unable to identify the single best parameter set, as the model performed well over a range of parameters. The evaluation also revealed differences in peak locations for each variable, complicating parameter optimization. Additionally, single-variable evaluations can lead to misleading conclusions, as performance improvements for one variable may degrade the performance of others, especially with less accurate topography data like SRTM. Later we performed a multivariable integrated evaluation using OSK metrics, integrating Q, WSE, and FA. Using OSK, the sensitivity of the parameter was reduced with one single optimal performance zone identified corresponding to best single parameter set for the MERIT DEM. It also confirms that with accurate topography data and a multivariable integrated evaluation approach, the river model can reduce the problem of equifinality, that is, multiple sets of similar performing parameters.

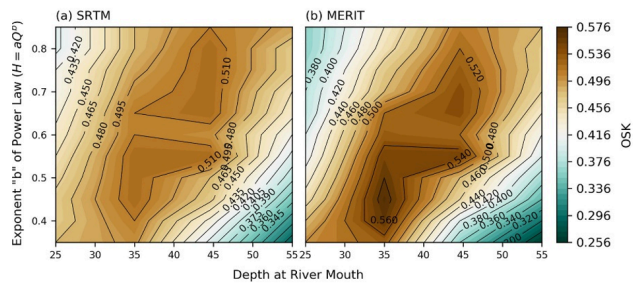


Figure 2: Overall basin skill score contour plot with equal weighting of all three variables (discharge (Q), water surface elevation, and flooded area) for (a) the Shuttle Radar Topography Mission (SRTM) digital elevation model (DEM) and (b) the Multi-Error-Removed Improved-Terrain (MERIT) DEM

Conclusion: The proposed multivariable integrated evaluation framework, using the OSK metric and NNSE, offers a more comprehensive assessment of hydrodynamic model performance by incorporating multiple variables and overcoming limitations of single-variable evaluation, such as equifinality and performance compensation. The method, applied to CaMa-Flood with SRTM and MERIT DEMs, highlighted improved accuracy with MERIT. This framework offers flexibility and reliability for large-scale river hydrodynamic model evaluation.

[B6] Correction of River Bathymetry Parameters Using the Stage–Discharge Rating Curve

Xudong Zhou et al. 2022, Water Resources Research, <https://doi.org/10.1029/2021WR031226>

Abstract: River bathymetry is an important parameter for hydrodynamic modeling; however, it is associated with large bias because direct large-scale measurements are impractical. Recent studies adjusted river bathymetry data based on assessment of the difference between modeled and observed water surface elevation (WSE); however, model uncertainties in river discharge can lead to unintended errors in correcting river bathymetry. In this study, we propose a simple but robust and rational correction method of river bathymetry using the bias between stage–discharge rating curves rather than WSE time series data. The rating curve represents the internal characteristics of the river section and is not sensitive to the instantaneous simulated discharge errors. Our results showed that the corrected river bathymetry are robust to bias in runoff as they converged among experiments driven by noise-corrupted or multi model runoff forcing. Evaluation with the corrected river bathymetry against virtual truth demonstrated that the new method reduced 0.85–1.12 m of the absolute bias than the result from the conventional method. The deviation among the results reduced by more than 70% particularly in river sections with no backwater effects. Evaluation of the corrected river model output also showed the advantage of rating-curve bias correction, as the simulated WSE is reasonably better only with better runoff, and it does not conceal errors in runoff inputs. Given the difficulty of eliminating discharge errors and bias in runoff, a method for correcting river bathymetry that is free from discharge and runoff errors is important for improving hydrodynamic modeling.

Introduction: River bathymetry is a critical parameter for hydrodynamic modeling, particularly for accurate simulations of water surface elevation (WSE). However, river bathymetry, which describes the underwater topography of river channels, is difficult to measure directly on a large scale, leading to significant biases in hydrodynamic models. Current global river models, such as CaMa-Flood and LISFLOOD-FP, approximate river bathymetry using empirical power-law relationships with climatological discharge. While these approximations capture large-scale patterns, they often require local calibration to reduce uncertainties. The correction of river bathymetry parameters in large-scale models is a well-studied problem, but existing methods often rely on observed WSEs and high-quality discharge simulations, which can introduce errors due to uncertainties in runoff and discharge modeling. This study proposes a new method for correcting river bathymetry using the stage-discharge rating curve, which is less sensitive to instantaneous discharge errors, making the correction more robust and independent of runoff uncertainties.

Methodology: The study introduces two methods for bias correction: the Time Series Method (TS-Method), which calculates the bias between simulated and observed WSE time series, and the Rating Curve Method (RC-Method), which uses the bias between stage-discharge rating curves derived from simulations and observations. The RC-Method is designed to be less sensitive to discharge errors, as the rating curve reflects the internal characteristics of the river section rather than instantaneous discharge. The study conducts three experiments: (1) using noise-corrupted runoff inputs to simulate discharge errors, (2) applying multiple model-based runoff inputs to represent more realistic runoff uncertainties, and (3) Observing System Simulation Experiments (OSSEs) to evaluate the accuracy of the corrected river

bathymetry against a virtual truth. The study area is the Amazon River Basin, where extensive discharge and WSE data are available from the Global Runoff Data Centre (GRDC) and HydroWeb.

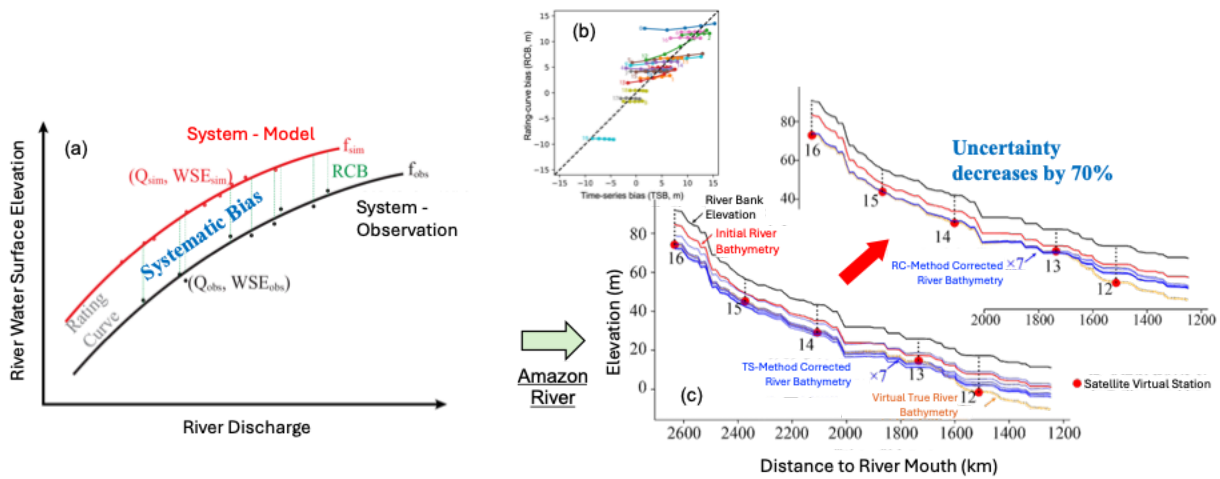


Figure. (a) the conceptual illustration of the rating-curve method to correct river bathymetry. (b) the implementation of the RC-Method to Amazon River basin, showing bias estimates using TS-Method and RC-Method. (c) the comparison between river bathymetry using two different methods.

Results: The results demonstrate that the RC-Method is robust to runoff uncertainties, as the corrected river bathymetry converges across different runoff inputs, unlike the TS-Method, which shows significant variation. In the noise-corrupted runoff experiment, the RC-Method consistently reduced WSE bias across all runoff inputs, while the TS-Method showed increased bias with higher runoff levels. The RC-Method also performed well in the multiple model-based runoff experiment, with corrected river bathymetry showing minimal divergence among different runoff inputs. In the OSSEs, the RC-Method corrected river bathymetry to closely match the virtual truth, particularly in river segments without backwater effects. The study found that the RC-Method reduced the absolute bias by 0.85–1.12 meters compared to the conventional TS-Method, with a 70% reduction in deviation among results. The RC-Method also improved the model's performance by ensuring that better runoff inputs led to better WSE simulations, without concealing errors in runoff.

Conclusion: The study concludes that the RC-Method provides a robust and rational approach for correcting river bathymetry in hydrodynamic models, independent of river discharge errors. Unlike the TS-Method, which is sensitive to runoff uncertainties, the RC-Method ensures that corrected river bathymetry is consistent across different runoff inputs, making it more reliable for large-scale applications. The RC-Method's performance is particularly strong in river segments without backwater effects, although further improvements are needed for backwater-affected sections. With the increasing availability of satellite altimetry and discharge data, the RC-Method offers a promising solution for improving hydrodynamic models, especially in data-scarce regions. Future work could focus on refining the method for backwater-affected rivers and exploring the sensitivity of the correction to river channel parameters such as shape and roughness coefficients.

2C: Achievements on CaMa-Flood applications

List of papers on CaMa-flood applications in 2022-2024

[C1] Quantifying the relative contributions of climate change and ENSO to flood occurrence in Bangladesh

Shahab Uddin, et al. 2023, Environmental Research Letters, <https://doi.org/10.1088/1748-9326/acfa11>

[C2] Uncertainty of internal climate variability in probabilistic flood simulations using d4PDF

Yuki Kita, & Dai Yamazaki, 2023, Hydrological Research Letters, <http://doi.org/10.3178/hrl.17.15>

[C3] Methodology for constructing a flood - hazard map for a future climate

Yuki Kimura, et al., Hydrology and Earth System Science, 2023. <http://doi.org/10.5194/hess-27-1627-2023>

[C4] Reconstruction of long-term hydrologic change and typhoon-induced flood events over the entire island of Taiwan

Jac Stelly, [Amar Deep Tiwari](#) et al., Journal of Hydrology: Regional Studies, 2024, <http://doi.org/10.1016/j.ejrh.2024.101806>

[C5] Climate change and urban sprawl: Unveiling the escalating flood risks in river deltas with a deep dive into the GBM river delta

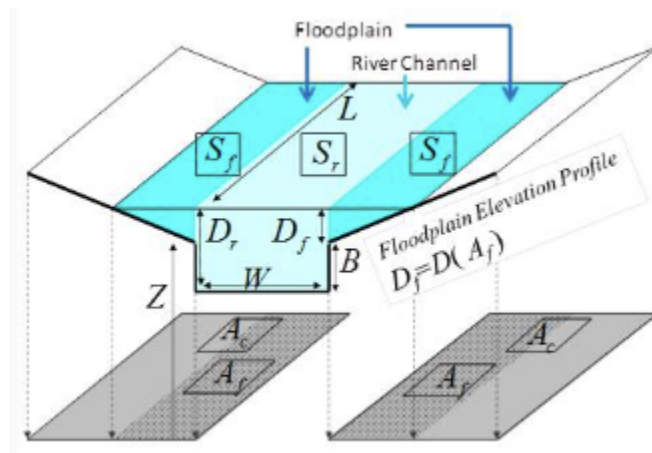
Shupu Wu et al., Science of the Total Environment, 2024, <http://doi.org/10.1016/j.scitotenv.2024.174703>

[C6] Substantial increase in future fluvial flood risk projected in China's major urban agglomerations

Ruijie Jiang et al. Communications Earth & Environment , 2023, <http://doi.org/10.1038/s43247-023-01049-0>

[C7] Flood risk assessment for Indian sub-continental river basins

Urmin Vegad et al. 2024, Hydrology and Earth System Sciences, <https://doi.org/10.5194/hess-28-1107-2024>



[C1] Quantifying the relative contributions of climate change and ENSO to flood occurrence in Bangladesh

Shahab Uddin, Menaka Revel, Prakat Modi and Dai Yamazaki
(Monash University / The University of Tokyo)

Environmental Research Letters, 2023, <https://doi.org/10.1088/1748-9326/acfa11>

Abstract: The impact of internal climate variability on flooding in Bangladesh remains unclear due to the limited observations. Here, we assess the impacts of ENSO and climate change on flood occurrence in Bangladesh using a large-ensemble climate simulation dataset (d4PDF) and a global river model (CaMa-Flood). After separating 6,000 years of simulation (100-member ensemble river simulations for 1950–2010) into El Niño, La Niña, and neutral years, we calculated the extent to which each ENSO stage increased flood occurrence probability relative to the neutral state using the fraction of attributable risk (FAR) method. In addition, we estimated the impact of historical climate change on past flood occurrence through comparison of simulations with and without historical global warming. Under the no-global-warming climate, La Niña increased the occurrence probability of a 10-year return period flood at Hardinge Bridge on the Ganges River by 38% compared to neutral years. Historical global warming increased the occurrence of flooding in the Ganges River, the Brahmaputra River, and their confluence by 59%, 44%, and 55%, respectively. The impact of ENSO on flood occurrence probability decreased in the historical simulation, likely due to the conflation of ENSO and climate change signals, and no significant correlation between ENSO and flood occurrence was detected when only small-ensemble simulations were used. These findings suggest that the use of large-ensemble climate simulation datasets is essential for precise attribution of the impacts of internal climate variability on flooding in Bangladesh.

Introduction: The variation in sea surface temperature (SST) pattern known as the El Niño–Southern Oscillation (ENSO) is a large-scale internal climate variability indicator with a considerable impact on global climate. Many rivers around the world exhibit clear relationships between ENSO and flooding. However, the relationship between ENSO and flooding in Bangladesh has been unclear in previous studies (See supplementary Table of Uddin et al., 2023). The precise mechanism through which the ENSO phase influences floods in Bangladesh remains elusive, possibly due to the limited amount of observational data available. The recurrence cycle of ENSO varies from 2 to 7 years and therefore drawing precise conclusions from an observational record that is only a few decades long is challenging. For this purpose, we quantified the impact of ENSO on flooding under historical (HIS) and no-global-warming (NAT) climate conditions and assessed the impact of climate change on flooding using large-ensemble climate simulation with the HIS and NAT datasets.

Methods: The CaMa-Flood hydrodynamic model was used in this study to simulate daily discharge at a spatial resolution of $0.25^\circ \times 0.25^\circ$. We performed a regional simulation for the Ganges–Brahmaputra–Meghna (GBM) basin. Three-hour average runoff data from d4PDF was used as the input. The simulation was run for 6,000 years under the HIS climate and another 6,000 years under the NAT climate. The flood occurrence probability was derived by determining the proportion of ensemble

members that exceeded the 10-year return period flood threshold. We used the probabilistic approach known as the fraction of attributable risk (FAR) method. FAR can measure the extent to which anthropogenic forcing contributes to flood occurrence. We used this to quantify the flood occurrence probability for the phases of ENSO (La Niña and El Niño).

Results: La Niña increased the occurrence probability of a 10-year return period flood at Hardinge Bridge on the Ganges River by 38% compared to neutral years in NAT climate. The influence of La Niña or El Niño state on flood occurrence probability in the Brahmaputra River at Bahadurabad station is negligible. Climate change increased the occurrence of flooding in the Ganges River, the Brahmaputra River, and their confluence by 59%, 44%, and 55%, respectively.

The impact of ENSO on flood occurrence probability decreased in the historical simulation, likely due to the conflation of ENSO and climate change signals. Here, we found that no significant correlation between ENSO and flood occurrence was detected when only small-ensemble simulations were used. We obtained stable correlations ($P < 0.05$) between ENSO and flood occurrence with ensemble sizes of around 1800 (30 perturbations of 60 years) and greater.

Conclusion: We assessed the contributions of ENSO and climate change to flood occurrence in Bangladesh using a large-ensemble climate simulation dataset (d4PDF) and the CaMa-Flood hydrodynamic model. While climate change had a clear impact of increasing flood occurrence probability throughout the Ganges–Brahmaputra River basin, we found that the occurrence of floods in the Ganges River also increased significantly in La Niña years. We found that a large-ensemble dataset is required to attribute floods in Bangladesh to the impact of ENSO.

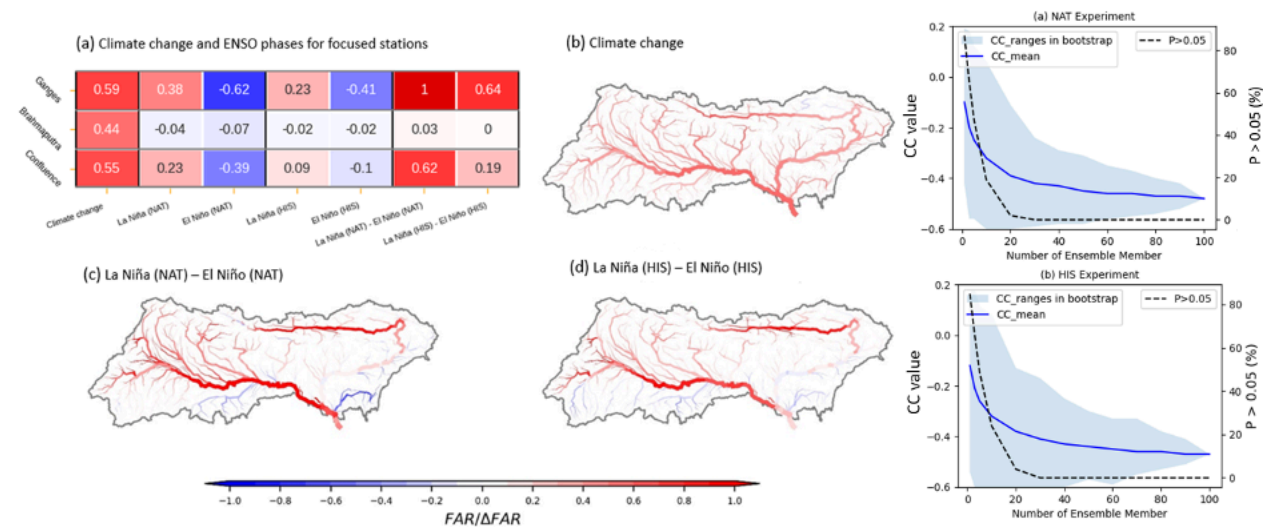


Figure: . Left panel: FAR values for the occurrence of a 10-year return period flood on the Brahmaputra and Ganges rivers attributed to climate change and ENSO. Figure (a) shows the results for the Hardinge Bridge (Ganges River), Bahadurabad (Brahmaputra River), and confluence sites, while figures (b–d) show results for the whole basin. Right Panel: Pearson's correlation coefficients and p-values between the 10-year return period flooding probability and ONI at Hardinge Bridge on the Ganges River for various ensemble sizes.

[C2] Uncertainty of internal climate variability in probabilistic flood simulations using d4PDF

Yuki Kita, Dai Yamazaki
(Gaia Vision Inc, Japan / The University of Tokyo)

Hydrological Research Letters, 17(2), p15-20, 2023, <http://doi.org/10.3178/hrl.17.15>

Abstract: We aim to evaluate the uncertainties associated with internal climate variability. We used large-ensemble river inundation simulations to quantitatively evaluate uncertainties in river depth and flood extent in the Yodo River basin. Using a single 60-year ensemble, the river depth for a 1,000-year return period (RP) flood scale have uncertainty between -11.7% and +9.2% in a 3,000-year flood simulation. To maintain the RP uncertainty within ± 300 years would require a simulation of $\geq 1,200$ years. The flood extent uncertainty with an RP of 1,000 years was found to be -8.4% and +7.6% based on a 3,000-year simulation for the basin. According to this result, the RP of the simulated flood extent ranges from 340–3,060 years. These results suggest that the decadal data used in conventional flood risk analyses potentially contain large uncertainty related to internal climate variability in the RP for water depth and flood extent by approximately 0.3–3-fold.

Motivation: The objective of this study was to quantitatively evaluate the uncertainty of extreme flood extents caused by internal climate variability. We calculated the uncertainty of extreme flood extents with a return period (RP) of 1,000 years, which are commonly used in flood hazard mapping. To evaluate uncertainties in the probability of recurrence of extreme events estimated from 60-year data, we used a 3,000-year dataset obtained from a large-ensemble hydrological simulation that is typically used in flood risk assessments based on limited past data. The results of this study demonstrate how uncertainties associated with the internal climate variability lead to large errors in the frequency of extreme river depth and flood extent values.

Method: For the large-ensemble hydrological simulation, we used the global riverine inundation model CaMa-Flood v4.04 (Yamazaki et al., 2011), and d4PDF (Mizuta et al., 2017) runoff dataset for the Japan region is used as input. The large-ensemble simulation was implemented with 50 members for 60 years individually. The resolution CaMa-Flood simulation was 1-arcmin and the resultant flood depth was downscaled into 1-arcsec (~30m) to obtain flood extents. We measure uncertainty in river depth and flood extent for each member of a 1,000-year RP flood compared to the entire 3,000-years extreme value (REF).

The Yodo River Basin in Japan was designated as the study target area. We validated the CaMa-Flood simulation results using annual maximum river discharge at a gauge station in the basin. We estimated an extreme value in flood extent using a Gumbel distribution.

Results: The annual maxima of river depth in the each member varied from -1.22 to $+0.96$ m, representing a variation of -11.7% and $+9.2\%$ with respect to the water depth of a 1,000-year RP flood in the reference experiment. A large uncertainty in flood extent was detected for a 1,000-year RP flood based on calculations from the each member, indicating that a simulation time of ≥ 1200 years is required to sufficiently reduce the uncertainty. The flood extent for a 1,000-year RP flood for the REF in the Yodo River basin was 351.7 km². Using a single 60-year simulation, the uncertainty of the flood extent of a 1,000-year RP flood was found to vary from -29.5 to $+26.7$ km² relative to that for the REF experiment, corresponding to a simulation period of 340–3060 years (Figure). As the simulation period increased to 300 and 1,200 years, the uncertainty of the flood extent of a 1,000-year RP flood decreased.

Decades of observational data and simulations used for conventional flood risk analysis have revealed potential overestimation of the RP for water depth and flood extent (by approximately 0.3–3-fold). For a 1,000-year RP flood extent, that uncertainty range corresponds to a recurrence period of 340–3060 years with a sufficiently long simulation period (3,000 years; REF). We performed a quantitative analysis of uncertainties in extreme river depth and flood extent using a large-ensemble hydrological CaMa-Flood simulation concerning internal climate variability. Despite limitations in the simulation model and analytical methods, our results clarify issues related to the internal climate variability caused by simulation time constraints, and will help improve the reliability of flood risk assessment maps in Japan.

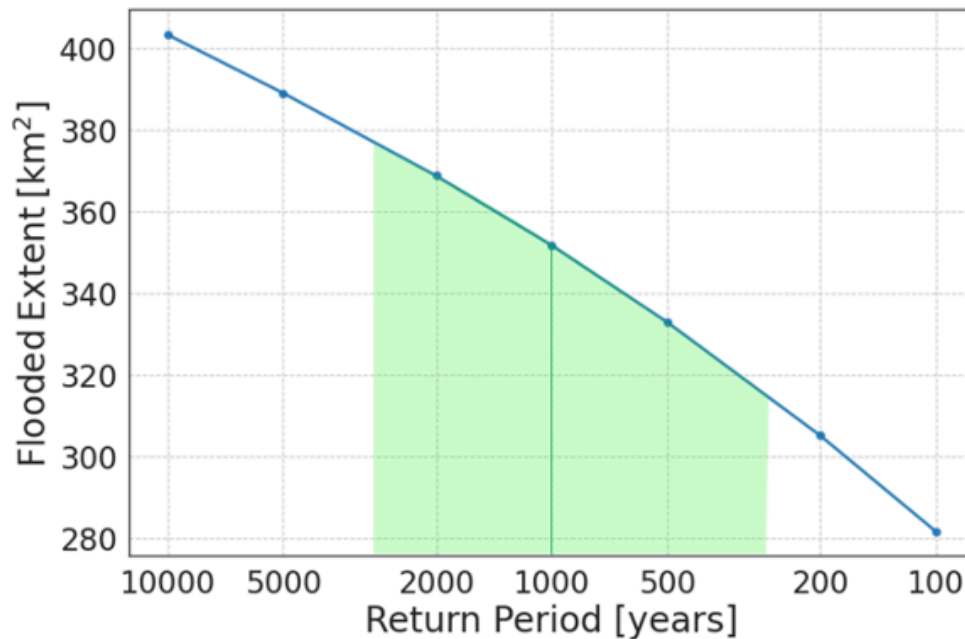


Figure. Probabilistic curve of flood extents for a 1,000-year RP flood for the REF experiment (blue line), and the corresponding return period (CRP) for the ORG experiment (green shading)

[C3] Methodology for constructing a flood hazard map for a future climate

Yuki Kimura 1 2 , Yukiko Hirabayashi 3 , Yuki Kita 2 4 , Xudong Zhou 5 , Dai Yamazaki 2

1 Risk Assessment Department, MS&AD InterRisk Research & Consulting, Inc.,

2 Institute of Industrial Science, The University of Tokyo

3 Department of Civil Engineering, Shibaura Institute of Technology

Hydrology and Earth System Science, 2023. <http://doi.org/10.5194/hess-27-1627-2023>

Abstract: Flooding is a major natural hazard in many parts of the world, and its frequency and magnitude are projected to increase with global warming. With growing concern about climate change, detailed and precise risk information is crucial for local countermeasures. However, the impacts of biases in climate-model outputs on river-flood simulation have not been fully evaluated, and thus evaluation of future flood risks using hazard maps (high-resolution spatial distribution maps of inundation depths) has not been achieved. Therefore, this study examined methods for constructing future-flood-hazard maps and discussed their validity. Specifically, we compared the runoff-correction method that corrects for bias in general-circulation-model (GCM) runoff using the monthly climatology of reanalysis runoff with the lookup method, which uses the GCM simulation results without bias correction to calculate changes in the return period, and depends on the reanalysis simulation to determine absolute flood depths.

The results imply that the runoff-correction method may produce significantly different hazard maps compared to those based on reanalysis of runoff data. We found that in some cases, bias correction did not perform as expected for extreme values associated with the hazard map, even under the historical climate, as the bias of extreme values differed from that of the mean value. We found that the change direction of a future hazard (increase or decrease) obtained using the runoff-correction method relative to the reference reanalysis-based hazard map may be inconsistent with changes projected by CaMa-Flood simulations based on GCM runoff input in some cases. On the other hand, the lookup method produced future-hazard maps that are consistent with flood hazard changes projected by CaMa-Flood simulations obtained using GCM runoff input, indicating the possibility of obtaining reasonable inundation-area distribution. These results suggest that the lookup method is more suitable for future-flood hazard-map construction than the runoff-correction method. The lookup method also has the advantage of facilitating research on efficient construction of future-climate hazard maps, as it allows for improvement of the reanalysis hazard map through upgrading of the model and separate estimation of changes due to climate change.

We discuss future changes at global scale in inundation areas and the affected population within the inundation area. Using the lookup method, the total population living in modeled inundation areas with flood magnitudes exceeding the 100-year return period under a future climate would be approximately 1.86 billion. In the assessment of future climate risks, we found that an affected population of approximately 0.2 billion may be missed if the historical hazard map is used as an alternative to constructing future-hazard maps and only frequency changes are considered. These results suggest that in global flood-risk studies, future-hazard maps are important for proper estimation of climate-change risks, rather than assessing solely changes in the frequency of occurrence of a given flood intensity.

Social Implementation of the future hazard map

Yuki Kimura^{1,2}; Yukiko Hirabayashi³; Dai Yamazaki¹ Email: ykimura@rainbow.iis.u-tokyo.ac.jp
¹The University of Tokyo, ²MS&AD InterRisk Research & Consulting, Inc., ³Shibaura Institute of Technology

Summary

- ❑ We have developed a global future flood hazard map by using a high-resolution terrain dataset based on satellite data and a global river inundation model. **The link to the paper with more details is as per the QR code.**
- ❑ This map has been publicly released to help society manage climate risks and is expected to be valuable in addressing climate change risks.
- ❑ We are planning to create a platform. This platform will allow users to easily access flood depth information and future flood risk information for their own locations.



Kimura et al. (2023), Methodology for constructing a flood-hazard map for a future climate. HESS, 27(5), 1627-1644

1. Description of global future flood hazard map

■ "Global Future Flood Hazard Map" – Access it for Free

MS&AD InterRisk Research & Consulting, Inc. have released the free future flood hazard map to the world from September this year.



■ "Global Future Flood Hazard Map" – Consulting version

MS&AD InterRisk Research & Consulting, Inc. commenced flood risk paid consulting services this April with more advanced specifications than the free version.

The consulting service supports the understanding of physical risks in the event of climate change, estimating the financial damages by flood and changes in inundation depth in the future.

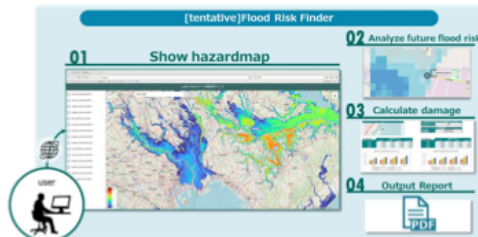
	Free version	Consultation version
Resolution	App. 500m	App. 90m
Return Period(RP)	RP100	RP100~1000
Year	2020, 2080	2020, 2030, 2050, 2080
SSP	ssp585	ssp126, ssp585
Region	Global	Global
Remarks	For non-commercial purposes only	-

2. Use case of the global flood hazard map

Use Case	Core Target
① TCFD disclosure	Calculate quantitative 'physical risk' in future climate -Companies supporting the TCFD
② Underwriting/Investment/loan portfolio verification	Consider the flood risk at the specific location when making underwriting, investment, and loan decisions. -Non-life -Bank -Investment Fund -Life insurers

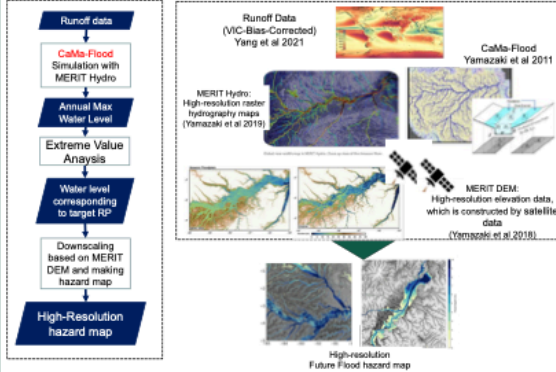
3. Future Plan

We will create the platform. An image of the platform is shown below. The platform allows users to check flood depth information for their own locations and to calculate the amount of flood damage(in current and future climate) by themselves.



4. Method to construct future flood hazard map

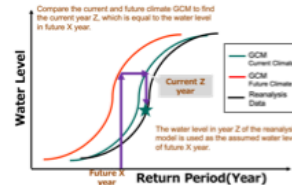
■ Generation of global flood hazard map



■ Method to construct the future flood hazard map

We use **Lookup method** to construct future flood hazard map.

Lookup method uses the GCM simulation results without bias correction to calculate changes in the return period, and depends on the reanalysis simulation to determine absolute flood depths.



We compared the result of Lookup method with the other method, which is the **runoff-correction method**

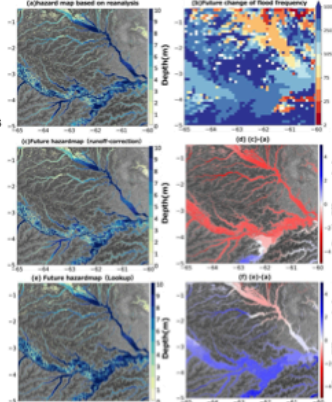
The method corrects for bias in general-circulation-model (GCM) runoff using the monthly climatology of reanalysis runoff, which is used for GCM bias correction in previous studies

5. Validation of the future flood hazard map

The hazard maps from the reanalysis and the Lookup method and "runoff-correction method" are shown in below Figure.

This Figure shows 100-year RP hazard map in Amazon River basin. In Figure b, blue indicates future flood hazard increase, red indicates decrease based on GCM simulation.

The runoff-correction method does not properly account for the changing trend of future flood hazard (Figure b) (Figure d). On the other hand, the Lookup method can construct future flood hazard maps that appropriately take into account the changing trends in future flood hazard (Figure f).



In aspect of consistency with trends in climate projection data, it is more reasonable to use the lookup method.

Acknowledgement

This research was supported by LaRC-Flood Project, which is the joint research project between the University of Tokyo, Shibaura Institute of Technology, MS&AD InterRisk Research & Consulting, Inc., and MS&AD Insurance Group Holdings, Inc.

[C4] Reconstruction of long-term hydrologic change and typhoon-induced flood events over the entire island of Taiwan

Jac Stelly^a, Yadu Pokhrel^a, Amar Deep Tiwari^a, Huy Dang^a, Min-Hui Lo^b, Dai Yamazaki^c, Tsung-Yu Lee^d
(^aMichigan State University, East Lansing, MI, United States; ^bNational Taiwan University, Taipei, Taiwan; ^cUniversity of Tokyo, Tokyo, Japan; ^dNational Taiwan Normal University, Taipei, Taiwan)

Journal of Hydrology: Regional Studies, 2024, <https://doi.org/10.1016/j.ejrh.2024.101806>

Abstract: This study presents long-term and high-resolution modeling of flood occurrence, interdecadal patterns of river-floodplain dynamics, and analysis of flooding during two typhoon events—Nari and Morakot over Taiwan. The modeling system combines a hydrological model (HiGW-MAT) and a river hydrodynamics model (CaMa-Flood), simulating hydrologic-hydrodynamic processes at ~ 5 km resolution with flood occurrences downscaled to ~ 90 m.

As the first investigation to conduct spatially comprehensive and temporally continuous modeling in Taiwan, this study presents important advances on the application of large-scale hydrological-hydrodynamic models in settings like that of Taiwan with important implications on flood prediction under climate change. The assessment of interdecadal changes in streamflow indicates no consistent trends over the past four decades; however, the variabilities in monthly-scale streamflow are significant and regionally diverse across Taiwan. Decadal changes in flood occurrence are also minimal at the island-scale, but the changes vary substantially across different regions and exhibit an increased variability over time. Furthermore, the simulated flood patterns in response to Typhoons Nari and Morakot suggest that the modeling framework can be used to reproduce the spatial dynamics and temporal progression of flooding under extreme events in relatively small regions like Taiwan.

Introduction: Climate change has intensified the global hydrological cycle, increasing the frequency of extreme hydroclimatic events such as heavy rainfall, floods, and prolonged droughts. Taiwan, located in a high tropical cyclone activity zone, experiences frequent typhoons that contribute significantly to its freshwater supply. However, changing storm dynamics have led to both excessive flooding and severe droughts. While research on Taiwan's typhoons and precipitation exists, studies on island-wide hydrologic impacts remain limited. Most hydrologic analyses focus on specific watersheds, largely in northern and southern Taiwan, with little attention to central and eastern regions. Additionally, reliance on point-based streamflow measurements poses challenges due to spatial and temporal inconsistencies. To address these gaps, this study employs an advanced hydrologic-hydrodynamic modeling framework using HiGW-MAT and CaMa-Flood. The research aims to reconstruct four decades of hydrologic changes and assess the models' ability to simulate floods during major typhoons, improving understanding of Taiwan's evolving hydroclimatic conditions.

Methodology: CaMa-Flood is a global hydrodynamic model widely used for simulating river-floodplain hydrodynamics. It employs unit catchments with discretized river and floodplain topography, improving flood depth simulations, particularly in regions with seasonal precipitation. This study uses default CaMa-Flood parameters to assess its performance and applies the local inertial equation to compute river

streamflow. HiGW-MAT, a global hydrological model, provides daily runoff input, with anthropogenic activities disabled to focus on natural flood conditions. The study runs CaMa-Flood version 4.0 at a 3-arcminute resolution over Taiwan from 1980 to 2016, with a five-year spin-up. Flood depth is downscaled to 3-arcsecond (90m at equator) resolution. Results are validated against Taiwanese Water Resource Agency hydrological data (streamflow) and Landsat-based water occurrence (water occurrence) datasets. This study enhances understanding of Taiwan's hydrodynamic changes, aiding future research on flood modeling and climate-driven hydrologic shifts.

Results: The HiGW-MAT and CaMa-Flood modeling framework has been validated globally, but this study provides the first application in Taiwan. Model performance is assessed at nine hydrological monitoring stations, comparing observed and simulated streamflow from 1980–2016. Results show high correlation ($R^2 > 0.9$ at multiple stations), reasonable percent bias (mostly within $\pm 25\%$), and strong Kling-Gupta Efficiency scores. Trends indicate increasing streamflow from

the 1980s to 2000s, followed by a decline in the 2010s, with peak flows varying across regions. Flood dynamics are validated against Landsat-based water occurrence data, revealing good spatial agreement despite minor discrepancies in small floodplains. Decadal analysis shows shifting flood occurrence patterns, with increases in the 1990s and 2000s followed by declines in the 2010s. Simulated flood depths during Typhoons Nari (2001) and Morakot (2009) closely match observed.

Conclusion: This study presents the first island-wide hydrologic and flood modeling for Taiwan using CaMa-Flood, capturing streamflow and flood dynamics over four decades. Results show substantial seasonal variability but no consistent long-term trend. The model effectively simulates historical floods and extreme typhoon events, despite uncertainties. Future studies can refine simulations by integrating coastal flooding and human activity influences.

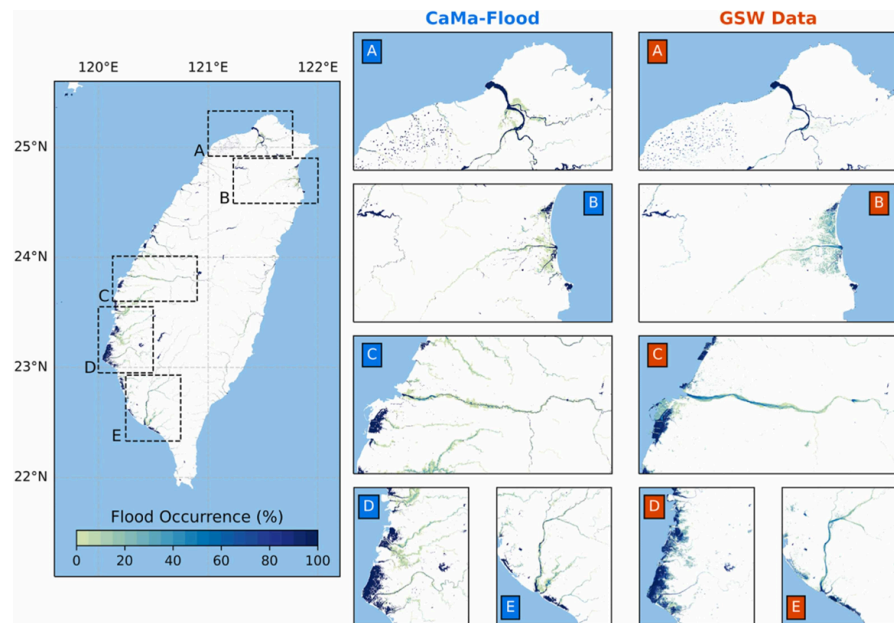


Figure 1. Spatial validation of CaMa-Flood simulated flood dynamics against GSW dataset.

[C5] Climate change and urban sprawl: Unveiling the escalating flood risks in river deltas with a deep dive into the GBM river delta

Shupu Wu et al., Science of the Total Environment, 2024, <http://doi.org/10.1016/j.scitotenv.2024.174703>

Shupu Wu ^a, Xudong Zhou ^b, Johan Reyns ^c, Dai Yamazaki ^d, Jie Yin ^a, Xiuzhen Li ^a

^a State Key Laboratory of Estuarine and Coastal Research, East China Normal University, Shanghai, China

^b School of Civil & Environmental Engineering and Geography Science, Ningbo University, Ningbo, China

^c Department of Water Science and Engineering, IHE Delft, Delft, the Netherlands

^d Global Hydrological Prediction Center, Institute of Industrial Science, The University of Tokyo, Tokyo, Japan

Abstract: River deltas, such as the Ganges-Brahmaputra-Meghna (GBM) delta, are highly vulnerable to flooding, exacerbated by intense human activities and rapid urban growth. This study explores the evolution of urban flood risks in the GBM delta under the combined impacts of climate change and urban expansion. Unlike traditional assessments that focus on a single flood source, we consider multiple sources—coastal, fluvial, and pluvial. Our findings indicate that future urban expansion will significantly increase flood exposure, with a substantial rise in flood risk from all sources by the end of this century. Climate change is the main driver of increased coastal flood risks, while urban growth primarily amplifies fluvial, and pluvial flood risks. This highlights the urgent need for adaptive urban planning strategies to mitigate future flooding and support sustainable urban development. The extreme high emissions future scenario (SSP5–8.5) shows the largest urban growth and consequent flood risk, emphasizing the necessity for preemptive measures to mitigate future urban flooding. Our study provides crucial insights into flood risk dynamics in delta environments, aiding policymakers and planners in developing resilience strategies against escalating flood threats.

1.Result

1.1 Changes in land cover and flood area during historical periods and future scenarios

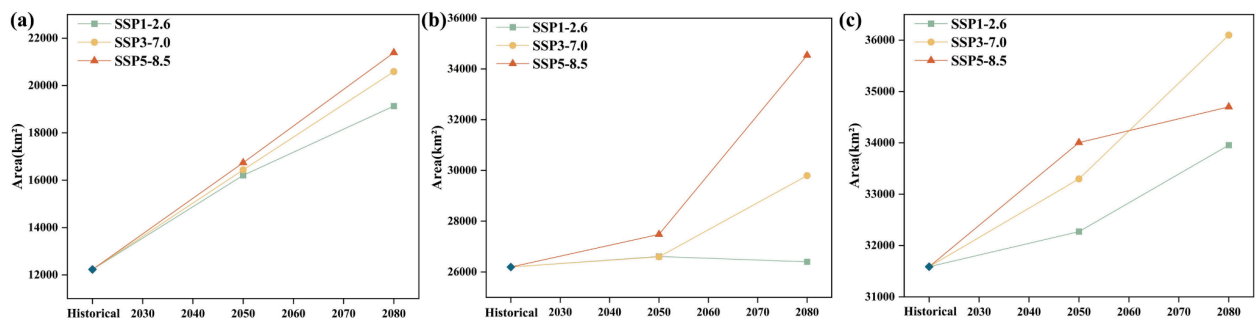


Figure 1. The variation in flood area for different types under historical periods and three scenarios (SSP1-2.6, SSP3-7.0, SSP5-8.5): (a) coastal floods, (b) fluvial floods, and (c) pluvial floods.

1.2 Changes in flood risk during historical periods and future scenarios

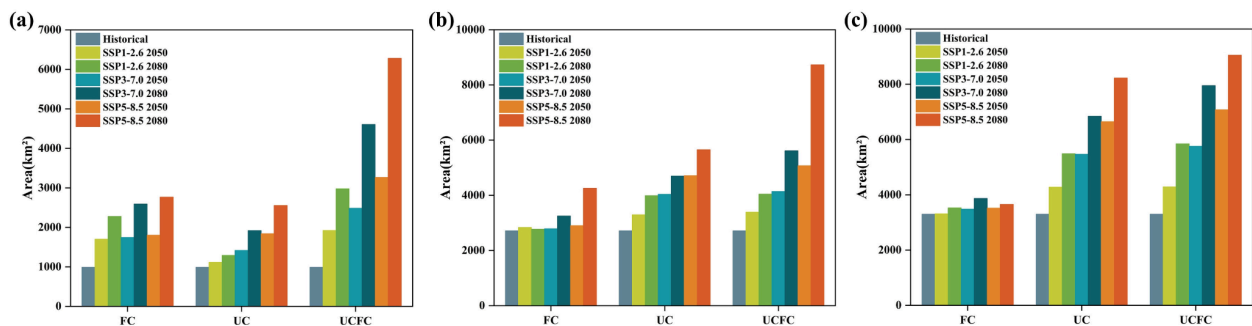


Figure 2. Urban flooded areas during historical periods and future scenarios: (a) coastal floods, (b) fluvial floods, and (c) pluvial floods; ‘FC’ denotes the condition where flood extents change while urban extents remain constant, ‘UC’ denotes the condition where urban extents change while flood extents remain constant, and ‘UCFC’ denotes the condition where both urban and flood extents change

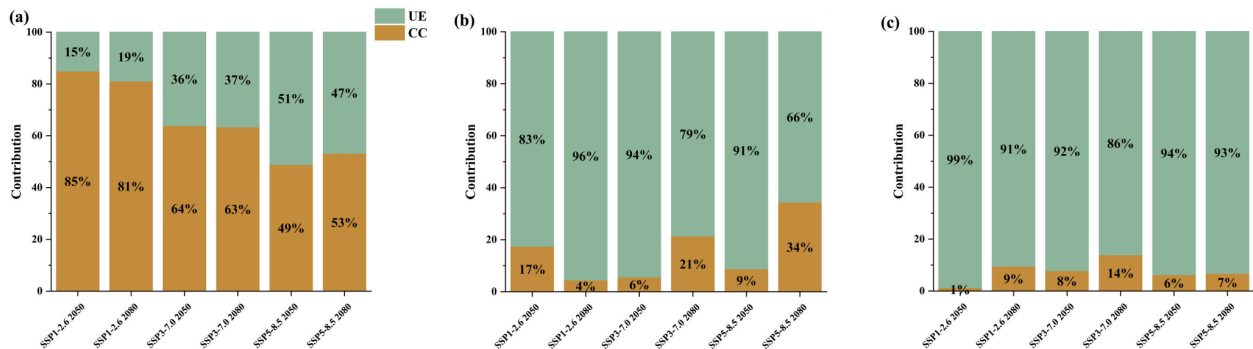


Figure 3. Contributions of climate change (CC) and urban expansion (UE) to the projected changes in inundated urban land areas (%): (a) coastal floods, (b) fluvial floods, and (c) pluvial floods

2. Conclusion

1. **Urban Expansion Trends:** Our study identifies a clear trend of increasing urban land area, particularly under the most extreme scenario, which predicts substantial growth by 2050 and 2080. This scenario forecasts that urban areas could nearly double in size, highlighting the pressing need for urban planning that accommodates such rapid expansion while mitigating potential flood risks

2. **Comprehensive Flood Risk Analysis:** We have discovered that traditional methods, which often focus on a single type of flooding, fall short in accurately predicting the complex nature of flood risks in river deltas. By analyzing various types of floods—pluvial, fluvial, and coastal—we've found significant differences in flood impacts, which emphasize the importance of a multifaceted approach in flood risk assessments to capture the true scope of risks.

3. **Scenario-Based Risk Projections:** Comparing different scenarios, it's clear that the most extreme scenario, which assumes more severe changes in climate and urban development, predicts larger areas affected by floods than the more moderate scenarios. This illustrates the potential impact of severe climate conditions and underscores the need for robust planning that can handle these extremes.

4. **Driving Factors Behind Increased Flood Risks:** Our findings underscore the dual impact of urban expansion and climate change as major drivers of increasing flood risks. While climate change intensifies coastal flood risks, urban growth contributes significantly to fluvial and pluvial flooding. This dual threat necessitates integrated strategies that consider both climate adaptation and urban development planning

[C6] Substantial increase in future fluvial flood risk projected in China's major urban agglomerations

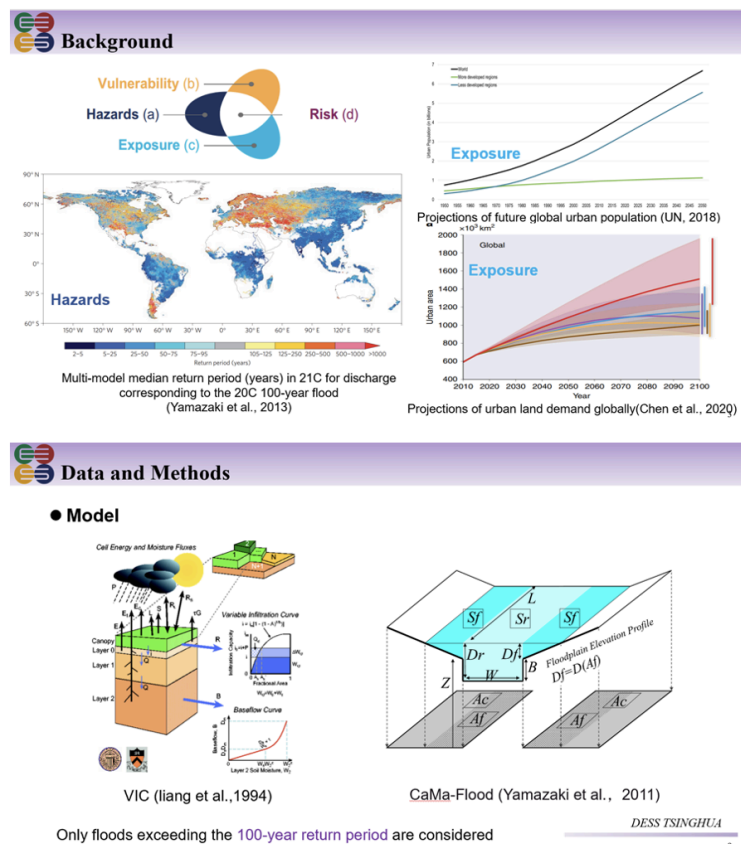
Ruijie Jiang, Hui Lu, Kun Yang, Deliang Chen, Wenyu Li, Nan Xu, Yuan Yang, Dabo Guan, Jiayue Zhou, Dai Yamazaki, Ming Pan, and Fuqiang Tian

(Tsinghua University / The University of Tokyo / University of California San Diego)

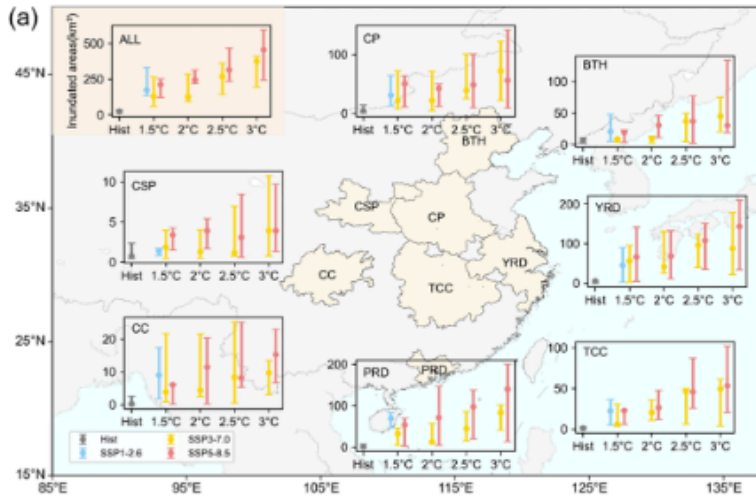
Communications Earth & Environment, 2023, <http://doi.org/10.1038/s43247-023-01049-0>

Abstract: Floods are one of the most destructive natural disasters and projecting future flood risk is essential for protecting lives and livelihoods. China is in the process of rapid urbanization, and most of the urban agglomerations are distributed on floodplains, facing high fluvial flood risk. The effect of urban spatial expansion, instead of densification of assets within existing urban cells, on flood risk has rarely been reported. Here, based on the latest projected urban land data and bias-corrected CMIP6 outputs, we project the future flood risk of seven urban agglomerations in China, home to over 750 million people.

The inundated urban land areas in the future are projected to be 4 to 19 times that at present, with southern China facing the greatest increase. Although climate change is the main driver for this strong projected rise in flood risk, the inundated urban land areas will be underestimated by 10-50% if the urban spatial expansion is not considered. Urban land is more likely to be inundated than non-urban land, and the newly-developed urban land will be inundated more easily than the historical urban land due to the marginal expansion of urban land. The results demonstrate the urgency of integrating climate change mitigation, reasonable urban land expansion, and increased flood protection levels to minimize the flood risk in urban land.



Results

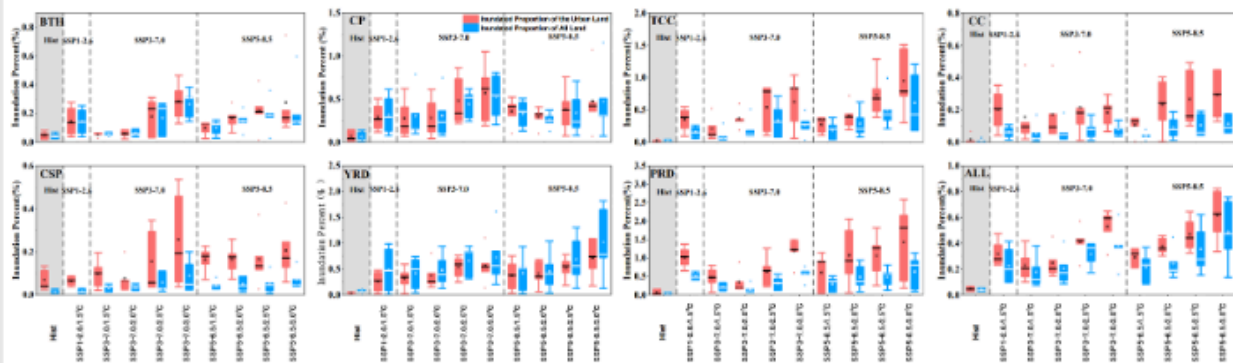


The 30-year average annual inundated urban land areas for the historical period and future warming levels under different scenarios.

- The flood risk of urban land is projected to rise significantly in the future
- Sharp rises after 2 °C warming in some urban agglomerations (e.g., YRD and TCC)
- The flood risk is the most extreme under SSP5-8.5

15

Results



The 30-year average annual inundated proportion of urban land (P_u , red) and total land (P , blue) of each urban agglomeration for the historical period and different warming levels under each scenario.

- the annual P_u is expected to rise to over 1% in TCC, YRD and PRD
- Urban land is more likely to be inundated

18

[C7] Flood risk assessment for Indian sub-continental river basins

Urmin Vegad¹, Yadu Pokhrel², and Vimal Mishra^{1,3}

(¹Civil Engineering, Indian Institute of Technology (IIT), Gandhinagar, India, ²Department of Civil and Environmental Engineering, Michigan State University, East Lansing, Michigan, USA, ³Earth Sciences, Indian Institute of Technology (IIT), Gandhinagar, India)

Hydrology and Earth System Sciences, 2024, <https://doi.org/10.5194/hess-28-1107-2024>

Abstract: Floods are among India's most frequently occurring natural disasters, which disrupt all aspects of socio-economic well-being. A large population is affected by floods during almost every summer monsoon season in India, leaving its footprint through human mortality, migration, and damage to agriculture and infrastructure. Despite the massive imprints of floods, sub-basin level flood risk assessment is still in its infancy and needs to be improved. Using hydrological and hydrodynamical models, we reconstructed sub-basin level observed floods for the 1901–2020 period. Our modelling framework includes the influence of 51 major reservoirs that affect flow variability and flood inundation. Sub-basins in the Ganga and Brahmaputra River basins witnessed the greatest flood extent during the worst flood in the observational record. Major floods in the sub-basins of the Ganga and Brahmaputra occur during the late summer monsoon season (August–September). Beas, Brahmani, upper Satluj, Upper Godavari, Middle and Lower Krishna, and Vashishti sub-basins are among the most influenced by the dams, while Beas, Brahmani, Ravi, and Lower Satluj are among the most impacted by floods and the presence of dams. Bhagirathi, Gandak, Kosi, lower Brahmaputra, and Ghaghara are India's sub-basins with the highest flood risk. Our findings have implications for flood mitigation in India.

Background

- To mitigate losses resulting from floods, the authorities must develop action plans and allocate sufficient funding. This can be achieved by identifying regions with a higher risk of flooding.
- A flood risk assessment performed on a global scale may not help in identifying the flood risk-prone regions at a country scale due to the coarser spatial resolution (Bernhofen et al., 2022).
- There have been studies on regional or river basin scales (Allen et al., 2016; Ghosh & Kar, 2018; Roy et al., 2021), but those do not provide flood risk at a sub-basin scale in India.
- Due to complex geomorphological characteristics and diverse climatic conditions, India is considered a relatively high flood-risk region (Hochrainer-Stigler et al., 2023).
- Therefore, estimating flood risk on a finer scale (e.g. sub-basin level) is essential for reliable flood risk assessment.

Science Questions

- How does the flood risk vary at the sub-basin scale in India during the 1901-2020 period?
- Which are the sub-basins where the presence of reservoirs considerably influences the flood risk?

Data and Methods

	Resolution	Source / Reference
Climate data		
Precipitation (IMD)	0.25° (~25km x 25km)	(Pai et al., 2014)
Temperature (IMD)	1.0°	(Srivastava et al., 2009)
Wind Speed (NCEP-NCAR)	1.875° x 1.905°	https://psl.noaa.gov/data/gridded/data.ncep.reanalysis.pressure.html
Population data		
Global Human Settlement Layers (GHSL)	30 arc-seconds	Joint Research Centre (JRC), 2021
Observed Flood Datasets	EM-DAT, DFO	

C-Ratio is a ratio of the total upstream reservoir volume to the mean annual discharge at a selected point along the river (Nilsson et al., 2005; Zajac et al., 2017).

Flood Risk is calculated as a function of vulnerability, hazard, and exposure.

Vulnerability is obtained for each district from the "Climate Vulnerability Assessment for Adaptation Planning in India" report

Hazard is calculated as the exceedance probability of a flooded area exceeding the 20-year return period threshold in the last 50 years

Exposure is the number of population counts exposed to the flood extent

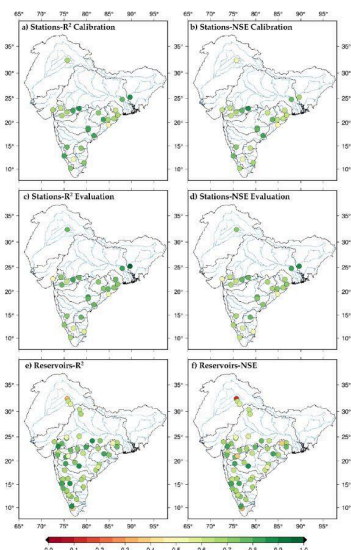


Fig 1: Calibration and evaluation of the combined model for daily river flow and reservoir storage at gauge stations and daily live storage of reservoirs

Model Framework and Calibration

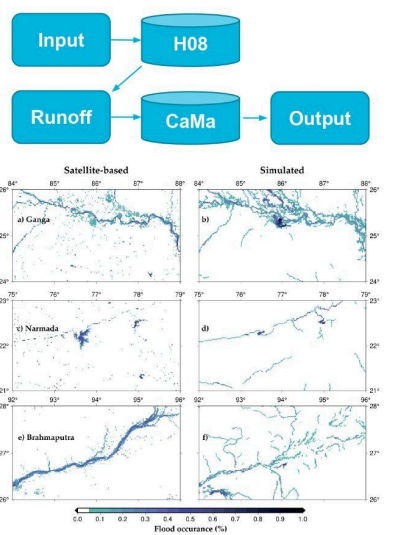


Fig 2: Simulated flood occurrences compared with satellite-based flood occurrence for different regions in Ganga, Narmada and Brahmaputra River basin

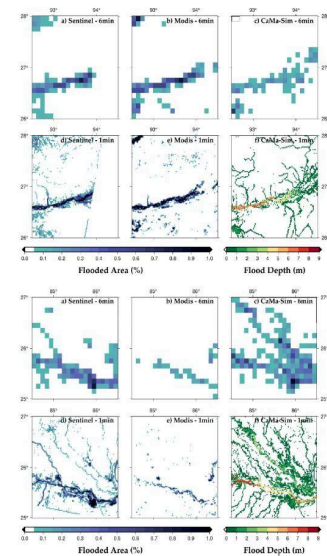


Fig 3: Simulated flood extent compared with Sentinel-1 SAR and MODIS satellite-based flood extent for two of the selected flood events

Key Results:

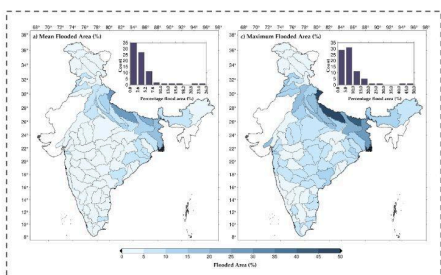


Figure 4: (a) Mean of annual maximum flooded area (percentage) between 1901-2020 and the overall distribution (c) Historical maximum flooded area (percentage) and the overall distribution

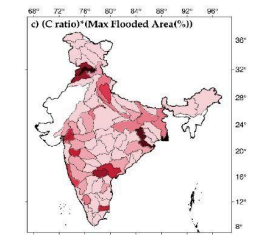
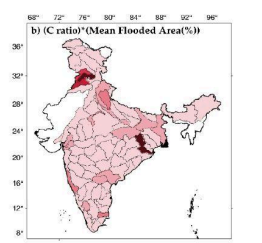
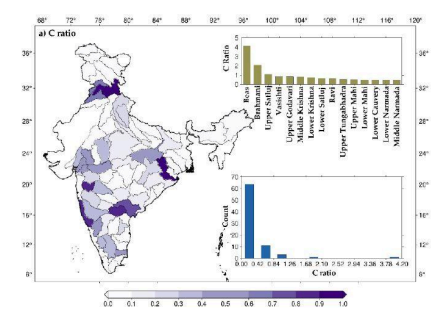


Figure 5: (a) Sub-basin wise C-ratio, top fifteen sub-basins and distribution of sub-basins based on C-ratio values (b) Mean of annual maximum flooded area (percentage) multiplied with C-ratio (c) Historical maximum flooded area (percentage) multiplied with C-ratio

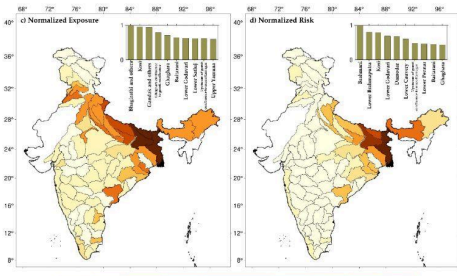
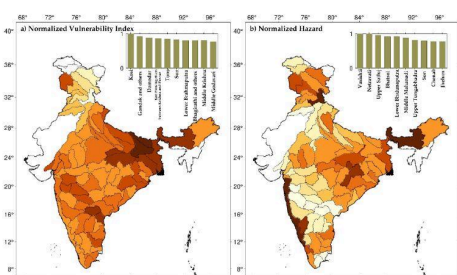


Figure 6: Sub-basin level (a) Normalized vulnerability index (b) Normalized hazard (c) Normalized exposure (d) Normalized risk. The top 10 sub-basins are highlighted as bars in panels inside the figures



2D Introduction of new data/tool helpful for CaMa-Flood

List of papers on new data/tools in 2022-2024

[D1] AllocateRiverGauge tool v1.0

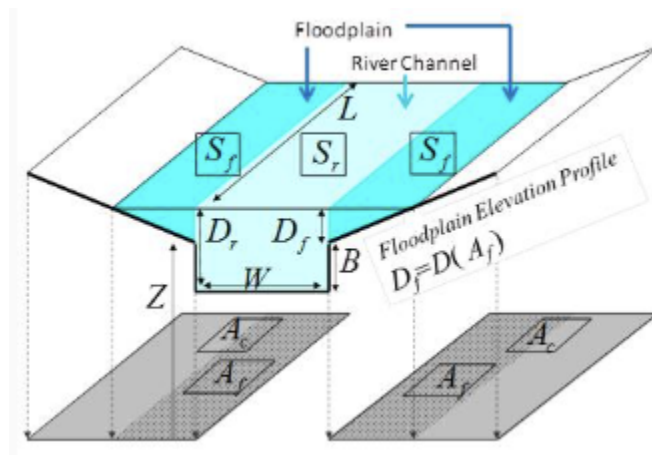
Yamazaki et al. 2024, GitHub, <https://github.com/global-hydrodynamics/AllocRiverGauge/>

[D2] AltiMaP: altimetry mapping procedure for hydrography data

Menaka Revel et al. 2024, Earth System Science Data, <https://doi.org/10.5194/essd-16-75-2024>

[D3] Res-CN (Reservoir dataset in China): hydrometeorological time series and landscape attributes across 3254 Chinese reservoirs

Youjiang Shen et al., Earth System Science Data, 2023. <https://doi.org/10.5194/essd-15-2781-2023>



[D1] AllocateRiverGauge tool v1.0

Dai Yamazaki, Menaka Revel, Xudong Zhou, and CaMa-Flood development tool

Institute of Industrial Science, UTokyo, Japan

Available on CaMa-Flood webpage and GitHub: <https://github.com/global-hydrodynamics/AllocRiverGauge/>

Abstract: Allocation of river gauges on model river network (i.e. finding a model grid corresponding to the observation gauge location) is essential for enabling comparison of observed and simulated water level. In order to make a precise and appropriate comparison between the observation and simulation, the gauge allocation should be done in a careful manner, considering potential errors in gauge attribute information and characteristics of modelled river network. We developed a tool to efficiently allocate gauges on CaMa-Flood network, and made it available as “**AllocateRiverGauge tool**”.

Basic strategy: We assume the information of latitude, longitude and upstream drainage area of river gauges is available hereafter (Lat, Lon, Uparea). We want to allocate these river gauges onto the model river network map (including CaMa-Flood and MERIT Hydro) by specifying the corresponding grid ID (iXX,iYY), in order to perform model evaluation using observed discharge and water level data.

However, it is complex to directly allocate river gauges onto a coarse-resolution river network map, as it's difficult to find the exact corresponding points on large-size grid boxes. Thus, the basic strategy is for gauge allocation consist of two steps:

[Step-1] allocate river gauges to high-resolution river map (30sec for global or 5sec for Japan)

[Step-2] calculate the corresponding grid on the coarse-resolution river map.

The high-resolution river maps (Global MERIT Hydro, YAMAZAKI ET AL. 2019; Japan J-FlwDir, YAMAZAKI ET AL. 2018) are prepared in this package. Users are expected to first allocate river gauges onto these maps.

Here, we need to assume that there might be:

[1] errors in reported data of each river gauge location (reported lat, lon, uparea)

[2] errors in high-resolution river network map. When these errors exist, river gauges might not be correctly allocated on the river map by automatic algorithm.

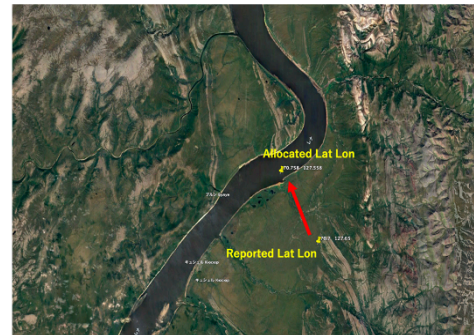
Thus, we recommend users to carefully check the automatic allocation results. If there is a suspicious data, please carefully examine the detail. You might need to [1] correct the reported info of some gauges, or [2] decide not to use the erroneous river gauges. This is why this allocation algorithm is treated as “SEMI-AUTOMATED”.

Once the gauges are allocated on high-resolution river map in [Step-1], secondary allocation of these gauges on coarse-resolution river maps can be automatically performed in [Step-2]. But please understand that some gauges on small rivers cannot be allocated on CaMa-Flood map, when these small rivers are not represented/resolved.

Step-1: Gauge allocation on MERIT Hydro

The pixel around the reported lat-lon location are searched within a search radius, and the allocation score is calculated as the sum of the uparea error and location error. The pixel showing minimum alloc_score is selected as “allocation point”. (For detail, see the manual)

Example of “Error in reported info, but correctly allocated”
ID=2903420 Kyusyur (Kusur) LENA RU



Step-2: Gauge allocation on CaMa-Flood map

Based on the location info (*Lat, Lon, Uparea*), this code searches the coarse-resolution grid which corresponds to the river gauges allocated on high-resolution river network map. Here, we consider the three types of correspondence between the coarse-resolution grid and the gauging station, depending on where the gauge exists on the sub-grid-scale river networks within each grid (see figure below).

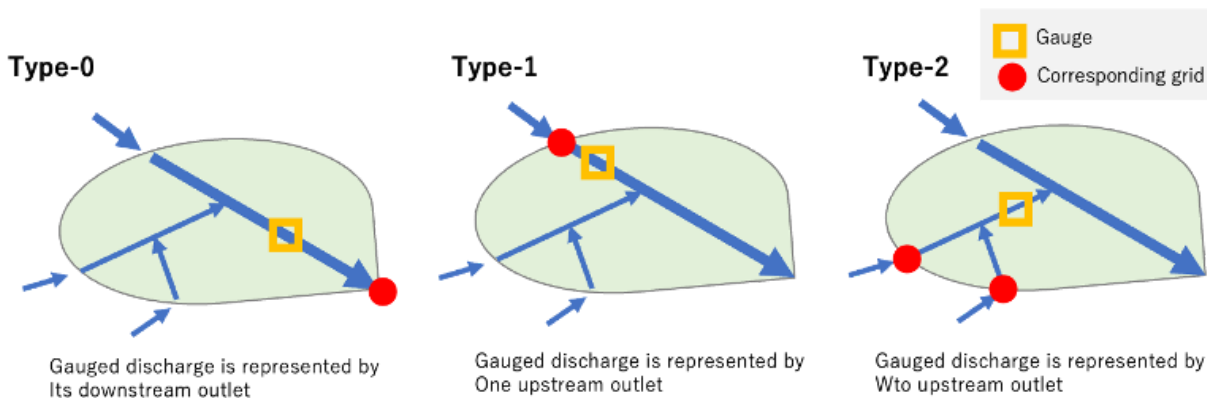


Figure: Sub-grid allocation strategy.

The sub-grid allocation strategy can be flexible, depending on the variable. For example for water level gauges, we also calculate the distance to upstream/downstream catchment outlets and elevation difference to them to consider possible interpolation of simulated water levels.

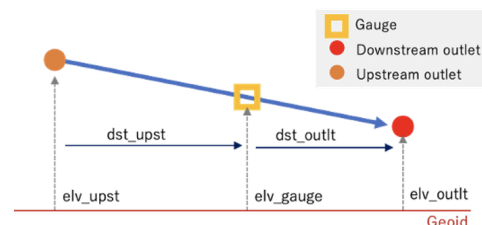


Figure: sub-grid information of the allocated water level gauge.

The AllocateRiverGauge tool package is available on CaMa-Flood webpage:

<https://hydro.iis.u-tokyo.ac.jp/~yamadai/cama-flood/>

[D2] AltiMaP: altimetry mapping procedure for hydrography data

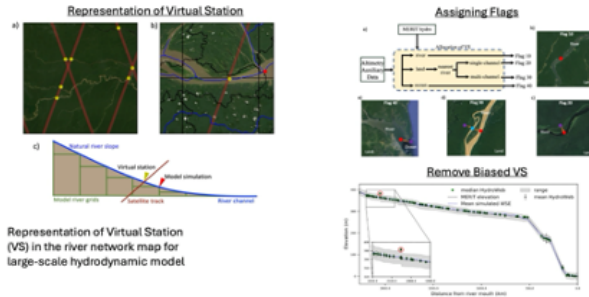
Menaka Revel, Xudong Zhou, Prakat Modi, Jean-François Cretaux, Stephane Calmant, and Dai Yamazaki

University of Waterloo, Canada / Institute of Industrial Science, UTokyo, Japan

Earth System Science Data, 2024, <https://doi.org/10.5194/essd-16-75-2024>

Abstract: Satellite altimetry data are important for monitoring water surface dynamics, assessing and calibrating hydrodynamic models, and improving river-related variables using optimization or assimilation techniques. However, comparing simulated water surface elevations (WSEs) with satellite altimetry data is difficult because the representative locations of satellite altimetry virtual stations (VSs) must be appropriately matched to the discrete river grids utilized in hydrodynamic models. In this study, we provide an automated altimetry mapping process (AltiMaP) for allocating VS sites from the HydroWeb database to the Multi-Error Removed Improved Terrain Hydrography (MERIT Hydro) river network. Each VS was assigned based on the land cover of the initial pixel allocation, with 10, 20, 30, and 40 indicating river channel, land with the nearest single-channel river, land with the nearest multi-channel river, and ocean pixels, respectively. Then, each VS was allocated to the closest MERIT Hydro river reach based on geometric distance. Out of the 12,000 allotted VSs, the majority (71.7%) were classified as flag 10. Flags 10 and 20 were primarily situated upstream and midstream, whereas flags 30 and 40 were primarily located downstream. Approximately 0.8% of VSs revealed bias, with significant elevation variations (≥ 15 m) between the mean observed WSE and the MERIT digital elevation model. These skewed VSs were primarily found in narrow rivers at high elevations. After employing AltiMaP for VS allocation, the simulated WSEs had a median root mean square error of 7.86 m compared to satellite altimetry data. The error rate improved significantly (10.6%) compared to a typical strategy, owing to bias reduction. Thus, assigning VSs to a river network using the proposed AltiMaP framework improves our comparison of WSEs predicted by the global hydrodynamic model to those acquired from satellite altimetry.

AltiMaP: Allocation, Removed Bias VS



AltiMaP: Data Description

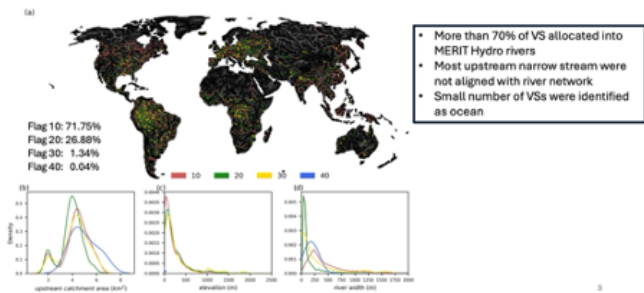
Variable	Description	Units
VS metadata		
ID	Identification number of VS	--
name	VS name	--
dataset	dataset name	--
long	longitude	degrees east
lat	latitude	degrees north
satellite	name of the satellite	--
MERIT Hydro-related		
flag	allocation flag	--
elevation	elevation at VS location on MERIT Hydro	m
dist_to_river	distance to the river catchment mouth	km
lx1	best x coordinate with respect to the $10^6 \times 10^6$ higher resolution tile	--
ly1	best y coordinate with respect to the $10^6 \times 10^6$ higher resolution tile	--
lx2	second best option of x coordinate with respect to the $10^6 \times 10^6$ high-resolution tile	--
ly2	second best option of y coordinate with respect to the $10^6 \times 10^6$ high-resolution tile	--
dist1	distance from the second best location to the VS	km
dist2	distance from the second best location to the VS	km
river_w	River width of the allocated location	m
Catchment resolution river network-related		
lx	x coordinate with respect to coarse resolution	--
ly	y coordinate with respect to coarse resolution	--
EDM20	EDM 20m datum elevation	m
EDM50	EDM 50m datum elevation	m

Details related to the VS metadata

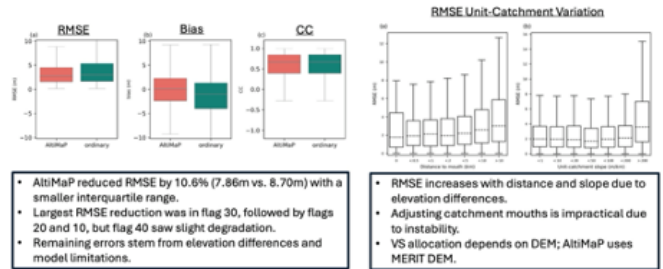
Allocation details related to the MERIT Hydro

Allocation details related to the CaMa-Flood river map

Characteristics of the allocation flags



Improvement by AltiMaP



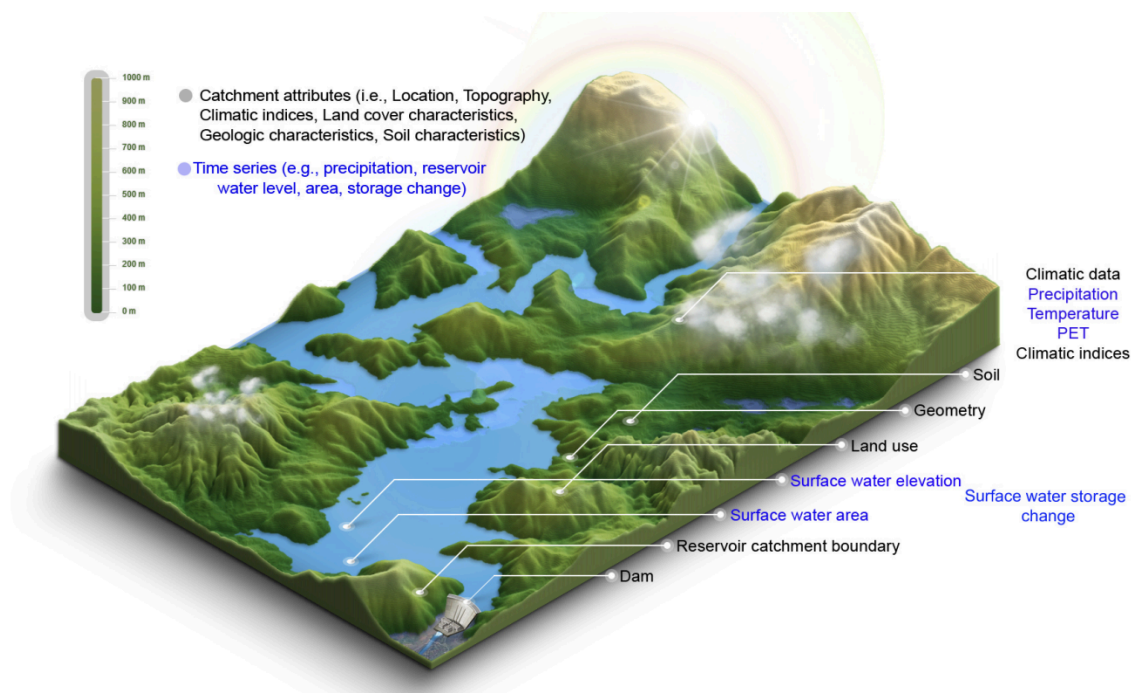
[D3] Res-CN (Reservoir dataset in China): hydrometeorological time series and landscape attributes across 3254 Chinese reservoirs

Youjiang Shen, Karina Nielsen, Menaka Revel, Dedi Liu, and Dai Yamazaki

Earth System Science Data, 2023. <https://doi.org/10.5194/essd-15-2781-2023>

Product Definition and Importance:

China's reservoir network, with over 98,000 dams and a total storage capacity exceeding 930 km³, plays a pivotal role in flood control, hydropower generation, and agricultural irrigation. However, the lack of a comprehensive, publicly available dataset on **reservoir-catchment characteristics** has hindered hydrological modeling and water resource management. Res-CN addresses this gap by providing hydrometeorological time series and landscape attributes for **3,254 Chinese reservoirs**, covering **73.2% of China's total reservoir storage capacity**. The dataset integrates multi-satellite observations (altimetry and optical imagery) and in-situ data to deliver detailed records of reservoir behavior and catchment characteristics from 1984 to 2021. Res-CN supports a wide range of applications, including **hydrological modeling, and water resource management**. **Repository: <https://zenodo.org/records/7664489>**.



Key Features:

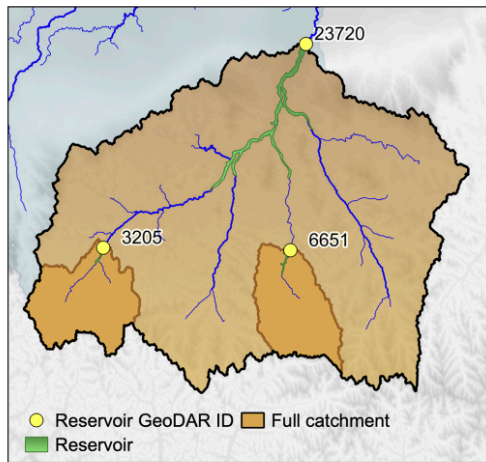
Comprehensive Reservoir-Catchment Attributes: Res-CN includes 512 attributes across six categories: reservoir and catchment body characteristics, topography, climate, soil and geology, land cover, and anthropogenic activities. These attributes are derived from high-quality satellite, reanalysis, and in-situ data, ensuring robust and reliable information for reservoir management and research.

Enhanced Satellite-Based Reservoir States: Water level: Data available for **20% of reservoirs**, with a 67% increase in spatial resolution. Water surface area: Coverage for **99% of reservoirs**. Storage anomaly:

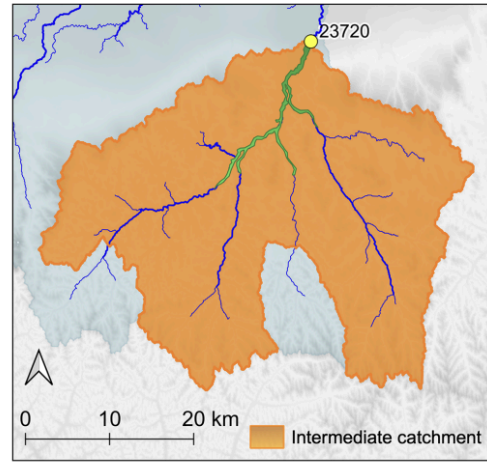
Coverage for **92% of reservoirs**, with a 225% increase in spatial resolution. Evaporation: Coverage for **98% of reservoirs**.

Dual Catchment Delineation:

a) Basin delineation A | Full catchments



b) Basin delineation. B | Intermediate catchments



Validation: The dataset includes detailed evaluation reports, providing transparency and reliability for users.

Open Access and Extensibility: Res-CN is freely available on Zenodo under a CC-BY license. The dataset includes Python, R, and Google Earth Engine (GEE) codes, allowing users to extend the inventory or apply the methods to other regions.

Product Examples

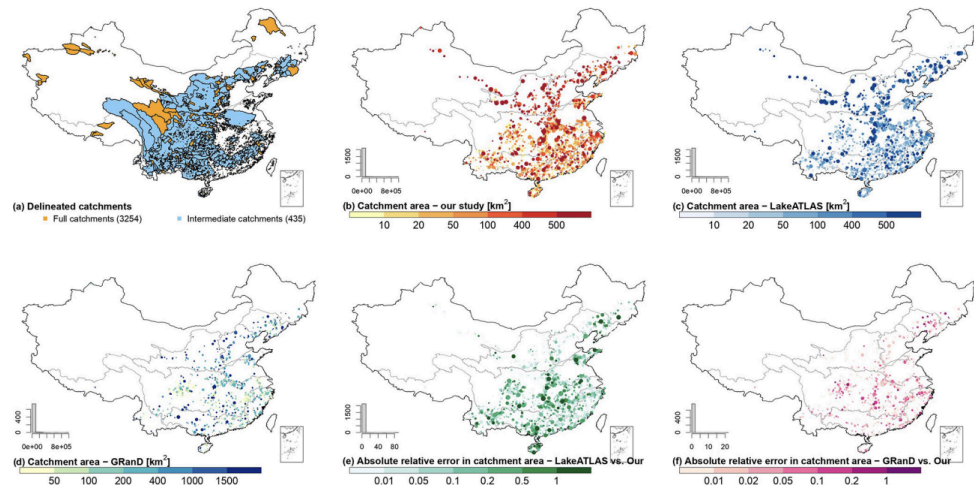
Future Plans:

Res-CN will be regularly updated to include new reservoirs and improved satellite data (e.g., from the SWOT mission).

Conclusion:

Res-CN represents a significant advancement in reservoir datasets, providing

comprehensive and high-quality data for 3,254 Chinese reservoirs. With its extensive catchment-level attributes, enhanced satellite-based reservoir states, and open-access design, Res-CN is a valuable resource for researchers, policymakers, and water managers. The dataset supports a wide range of applications, from hydrological modeling to climate research, and contributes to a better understanding of reservoir impacts on the Earth system.



3. Info on CaMa-Flood events and upcoming schedules

[X1] Next CaMa-Flood meetings

We are planning to have the 2nd CaMa-Flood user/developer meeting, possibly in September 2026 in the United Kingdom. The details will be announced when the meeting detail is decided.

In addition, we will organize the CaMa-Flood annual progress briefing every year (planned to be in every March), online on Zoom. If you have publications using CaMa-Flood in 2025, please consider joining this briefing, and share your contribution with CaMa-Flood community.

[X2] CaMa-Flood user/developer meeting (July 2024)

We held the first ever CaMa-Flood developer/user conference in July 2024. The meeting summary is available here:

<https://global-hydrodynamics.github.io/cmf-meet-2024/>

The international workshop "CaMa-Flood Developer/User Meeting 2024" for users and developers of the global river model CaMa-Flood was held on Friday and Saturday, July 5-6, 2024, at the Convention Hall of the Institute of Industrial Science, The University of Tokyo (IIS, The University of Tokyo).



This workshop was organized by Yamazaki Lab, the primary model development center of CaMa-Flood, to commemorate the 15th anniversary of the model's development since 2009. The global river model CaMa-Flood is widely used by research institutions and meteorological forecasting agencies both domestically and internationally. A total of 83 participants gathered, including 34 from 11 countries overseas and 49 from within Japan.

The keynote speech was delivered by Associate Professor Dai Yamazaki, who reflected on the 15-year history of model development. Following that, there were 23 oral presentations and 15 poster presentations divided into 8 sessions on the latest developments and cutting-edge applications of the global river model. In addition to introducing the latest research findings, there was active discussion among participants regarding future development directions.

This workshop successfully created a community of CaMa-Flood users, who had previously been conducting research individually, and it is expected to greatly accelerate future research and development.

CaMa-Flood user/developer meeting Awards

Based on the votes by all participants, three presenters are awarded for their huge contribution to CaMa-Flood modelling community.

=== CaMa-Flood best developer award ===

Shengyu Kang (Wuhan University)

A Computationally-efficient practice for global river hydrodynamic models

=== CaMa-Flood best user/application award ===

Michel Wortmann (ECMWF)

CaMa-Flood as part of the ECMWF Integrated Forecasting System

=== CaMa-Flood early career award ===

Mizuki Funato (The University of Tokyo)

Development of a Modified Reservoir Operation Scheme for Improved Global Flood Modeling





[X3] AOGS Large-scale River Modelling session (July-Aug 2025)

We will organize a Large-scale River Modeling session in AOGS 2025.

The meeting is from 27 July to 1 August in Singapore. Please consider joining, and I'm looking forward to meeting you there. [AOGS2025 meeting webpage](#)

The abstract submission deadline is 18 February.

(Session Info)

HS09: Advances in Large-scale River Modeling: Developments and Applications

Conveners:

Dr. Dai Yamazaki (The University of Tokyo)

Dr Peirong Lin (Peking University)

Dr Fitsum Woldemeskel (Bureau of Meteorology)

Dr Xudong Zhou (Ningbo University)

Scope:

Large-scale river modeling has continuously evolved in recent years. This evolution is due to many factors such as better conceptualization of river flow physics, new schemes to represent river infrastructures, advancement of baseline geography data like elevation and river networks, and increasing computational resources. These advancements enabled more advanced applications of large-scale river models, such as global-scale flood risk assessment, real-time flood forecast on the continental scale, coupling with Earth system models, and integration of satellite river observations into models through data assimilation. In this session, we welcome any research topics related to the development and/or applications of large-scale river models. New scientific discoveries obtained from large-scale river modeling and/or local decision-support applications are also welcome to submit. We will review the frontier research on large-scale river modeling and discuss next challenges and future directions.



CaMa-Flood annual briefing: Logistics

Organizing Committee

As of January 2025

- Dai Yamazaki (Chair, UTokyo)
- Zhou Xudong (Ningbo Univ)
- Gang Zhao (Science Tokyo)

Please email to Dai Yamazaki (yamada [at] iis.u-tokyo.ac.jp) and/or Xudong Zhou (x.zhou [at] rainbow.iis.u-tokyo.ac.jp) for question about the meeting.